Universidade de Aveiro Departamento de Ciências Médicas

2019

ALEXANDRE MIGUEL MANANA NUNES

Estudo da interação entre o vírus da influenza A e as enzimas modificadoras dos ARN de transferência

Unravelling the interplay between influenza A virus and transfer RNA-modifying enzymes

Universidade de Aveiro Departamento de Ciências Médicas

2019

ALEXANDRE MIGUEL MANANA NUNES

Estudo da interação entre o vírus da influenza A e as enzimas modificadoras dos ARN de transferência

Unravelling the interplay between influenza A virus and transfer RNA-modifying enzymes

Tese submetida à Universidade de Aveiro para cumprimento dos requisitos necessários à obtenção do grau de Mestre em Biomedicina Molecular, realizada sob a orientação científica da Doutora Daniela Maria Oliveira Gandra Ribeiro, Investigadora Auxiliar do Departamento de Ciências Médicas e Investigadora Principal do "Virus Host-Cell Interactions Laboratory" do Instituto de Biomedicina (iBiMED), Departamento de Ciências Médicas, Universidade de Aveiro e da Doutora Ana Raquel Santos Calhôa Mano Soares, Investigadora Doutorada do Instituto de Biomedicina (iBiMED), Departamento de Ciências Médicas, Universidade de Aveiro.

Thesis submitted to the University of Aveiro to fulfil the requirements to obtain the Master degree in Molecular Biomedicine, held under the scientific guidance of Dr Daniela Maria Oliveira Gandra Ribeiro, Assistant Researcher at the Department of Medical Sciences and Principal Investigator of the Virus Host-Cell Interactions Laboratory at the Institute of Biomedicine (iBiMED), Department of Medical Sciences, University of Aveiro and Dr Ana Raquel Santos Calhôa Mano Soares, Young Principal Investigator at the Institute of Biomedicine (iBiMED), Department of Medical Sciences, University of Aveiro .

This work was supported by the Portuguese Foundation for Science and Technology (FCT): PTDC/BIACEL/31378/2017 (POCI-01-0145-FEDER-031378), POCI01-0145-FEDER-016630, CEECIND/03747/2017, UID/BIM/04501/2013, POCI-01-0145-FEDER-007628 under the scope of the Operational Program "Competitiveness and internationalization", in its FEDER/FNR component.

It was also funded by the Comissão da Região Centro CCDRC and FEDER through the integrated project pAGE - CENTRO-01-0145-FEDER-000003.

This work was also supported by national funds (OE), through FCT, I.P., in the scope of the framework contract foreseen in the numbers 4, 5, and 6 of the article 23, of the Decree-Law 57/2016, of August 29, changed by Law 57/2017, of July 19

Image acquisition was performed in the LiM facility of iBiMED, a node of PPBI (Portuguese Platform of BioImaging): POCI-01-0145-FEDER-022122.

o júri

presidente

Doutora Sandrina Nóbrega Pereira
Professora Auxiliar Convidada do Departamento de Ciências Médicas da Universidade de Aveiro

Doutora Daniela Maria Oliveira Gandra Ribeiro
Investigadora Auxiliar do Departamento de Ciências Médicas da Universidade de Aveiro

Doutora Ana Sofia Paulo Varanda
Investigadora Doutorada do Centro de Neurociências da Universidade de Coimbra

agradecimentos

Antes de mais, um enorme agradecimento para todas as pessoas que me ajudaram, apoiaram e deram força durante toda esta etapa, porque sem elas não teria sido possível finalmente chegar ao fim.

Um obrigado às Dras. Daniela Ribeiro e Ana Raquel Soares, por me terem ajudado a dar os primeiros passos na investigação, por me terem sugerido o projeto e por me terem acompanhado ao longo do desenvolvimento deste.

Um obrigado à Rita, ao Bruno, à Jéssica, à Carolina, à Marisa, à Diana e a todos os outros membros do laboratório que me ajudaram ao longo de todos estes meses.

Um especial e grande obrigado à Mariana por todo o conhecimento e experiência que partilhou comigo, por toda a paciência que teve para responder às imensas perguntas que lhe fiz e acima de tudo por todas as horas que passou a ensinar-me como trabalhar em laboratório e a ajudar-me neste projeto.

Um obrigado a todos os meus colegas de mestrado que comigo partilharam estes anos e esta experiência.

Um obrigado a todos os meus amigos, em especial ao João e ao Rui, que sempre me apoiaram e deram palavras de incentivo durante todo este tempo.

E por fim, um grande e enorme abraço e obrigado para os meus pais, irmão, avós e avôs por tudo o que fizeram e fazem por mim. Por sempre me apoiarem e por estarem sempre presentes para me ajudarem. Sem vocês, isto nunca teria sido possível.

palavras-chave

Vírus da Influenza A, Infeção Viral, Proteostase, Interação Vírus-Hospedeiro, ARN de Transferência (ARNt), Modificações dos ARNt, Enzimas modificadoras do ARNt

resumo

Os vírus, como por exemplo o vírus da influenza A (VIA), são os agentes causadores da maior parte das epidemias respiratórias anuais em seres humanos: apoderam-se e controlam a maquinaria das células hospedeiras e estabelecem interações precisas com múltiplos componentes celulares, a fim de se propagarem. A razão fundamental pela qual os vírus precisam de células vivas para se multiplicarem, é o facto de não possuírem componentes fundamentais necessários para a replicação, como por exemplo, os ácidos ribonucleicos de transferência (ARNt). Alguns estudos demonstraram que o VIA manipula as populações de ARNt de células hospedeiras de forma a induzir a tradução eficiente de proteínas virais. Os ARNt são modificados, pós-transcrição, por enzimas modificadoras de ARNt (EMTs) de forma a garantir a estabilidade dos ARNt e que a tradução ocorra da forma mais eficiente possível. A maioria dessas modificações ocorre na posição 34 dos ARNt, localizada no anti codão, embora essas modificações também ocorram em outras áreas da estrutura dos ARNt.

Neste estudo, procurámos determinar se a infeção pelo VIA levava a alterações na expressão dos genes que codificam para as EMTs. Os resultados obtidos demonstraram que alguns genes (ELP1, ELP3, ELP6, ALKBH8 e TRMT2A) estavam a ser sobre-expressos duas horas após a infeção, enquanto nenhuma outra mudança significativa foi detetada em outros momentos.

Para além disso procurámos também determinar se a falta de ELP3 influenciaria de alguma forma a produção de partículas virais pelas células infetadas. Resultados preliminares obtidos usando células knockout para ELP3, indicam que a ausência dessa enzima reduz notavelmente a produção viral, sugerindo um papel relevante para a ELP3 no ciclo de vida do VIA.

keywords

Influenza A Virus (IAV), Virus Infection, Proteostasis, Virus-Host Interactions, Transfer RNA (tRNA), tRNA Modifications, tRNA-Modifying Enzymes

abstract

Viruses, such as the influenza A virus (IAV), are the causative agent for most of the annual respiratory epidemics in humans, and they take control of the host cell machinery and establish precise interactions with cellular components in order to propagate. The fundamental reason why viruses need living cells to multiply, is because they lack key elements that are needed for replication such as transfer ribonucleic acids (tRNAs).
IAV has been shown to specifically manipulate the host-cell tRNA population to enable the efficient translation of viral proteins. tRNAs are modified, post-transcriptionally, by tRNA-modifying enzymes (TMEs) to ensure their stability and efficient translation. The majority of these modifications occurs at the wobble position, located at the anticodon loop, although they may also happen in other areas of the tRNA structure.

In this study we aimed to determine whether IAV infection leads to changes in the expression of the genes that code for the TMEs. Our results demonstrated that particular genes (ELP1, ELP3, ELP6, ALKBH8 and TRMT2A) were overexpressed two hours post-infection while no striking changes were detected in other time points.

We also aimed to determine whether the lack of ELP3 would influence the viral particle production by the infected cells. Using ELP3 knockout cells, our preliminary results show that the absence of this TME notably reduces viral production, suggesting a relevant role for ELP3 on the IAV life-cycle.

List of abbreviations

aa-tRNA	aminoacyl-tRNA
ALKBH8	AlkB Homolog 8
ALS	Amyotrophic lateral sclerosis
AMP	Adenosine monophosphate
ATP	Adenosine triphosphate
BSA	Bovine serum albumin
CARD	Caspase activation recruitment domain
CCA	Cytosine-Cytosine-Adenine
cDNA	Complementary DNA
cRNA	Complementary RNA
DAPI	4′,6-diamidino-2-phenylindole
ddH_20	Double-distilled water
DMEM	Dulbecco's Modified Eagle Medium
DMSO	Dimethyl Sulfoxide
DNA	Deoxyribonucleic acid
dsRNA	double stranded RNA
ELB	Empigen Lysis Buffer
ELP1	Elongator complex protein 1
ELP3	Elongator complex protein 3
ELP6	Elongator complex protein 6
ER	Endoplasmic Reticulum
FBS	Fetal Bovine Serum
GAPDH	Glyceraldehyde 3-phosphate dehydrogenase
GC	Guide C
HA	Hemagglutinin
HIV-1	Human immunodeficiency virus type 1
HPI	Hours post infection
IAV	Influenza A Virus
IFN	Interferons
IFN-β	interferon-β
IGC	Instituto Gulbenkian de Ciência
IL	Interleukin
IRF	Interferon regulatory factor
KO	Knock Out
LysRS	Lysyl-tRNA synthetase
M2	Matrix 2
M^5U	5-methyluridine
MAVS	Mitochondrial antiviral signalling proteins
Mcm^5	5-methoxycarbonylmethyl
Mcm^5s^2U	5-methoxycarbonylmethyl-2-thiouridine
MOI	Multiplicity of Infection
mRNA	Messenger RNA
NA	Neuraminidase
NCBI	National Center for Biotechnology Information
Ncm^5	5-carbamoylmethyl

ncRNAs	Non-coding RNAs
NEP	Nuclear export protein
NF-kB	Nuclear factor kappa-light-chain-enhancer of activated B cells
NK	Natural Killer
NLRP3	NOD-like receptor family pyrin domain-containing-protein-3
NLS	Nuclear Localization Signals
NP	Nucleoprotein
NS1	Non-structural protein 1
NS2	Non-structural protein 2
P/S	Penicillin/Streptomycin
PA	Acidic polymerase
PAMP	Pathogen Associated Molecular Patterns
PB1	Basic polymerase 1
PB2	Basic polymerase 2
PBS	Phosphate Buffered Saline
PEI	Polyethylenimine
PFA	Paraformaldehyde
PFU/ml	Plaque forming units per milliliter
PP	Pyrophosphate
PRR	Pathogen Recognition Receptors
RIG-I	Retinoic acid-inducible gene-I
RNA	Ribonucleic Acid
RNP	Ribonucleoproteins
RPM	Rotations per minute
RT-qPCR	Reverse Transcription-Quantitative Polymerase Chain Reaction
Scr	Scramble
SD	Standard deviation
SFM	Serum Free Media
ssRNA	Single-stranded RNA
TBK1	TANK-binding kinase 1
TBS-T	Tris Buffered Saline with Tween 20
tiRNAs	stress-induced tRFs
TLE	Toll-like receptor
TME	tRNA-Modifying Enzymes
tRFs	tRNA fragments
TRIF	TIR-domain-containing adapter-inducing interferon-β
TRMT2A	tRNA methyltransferase 2 homolog A
tRNAs	transfer ribonucleic acids
UPR	Untranslated protein response
URM1	Ubiquitin-related modifier 1 protein
vRdRp	Viral RNA dependent RNA polymerase
vRNA	Viral RNA
vRNPs	Viral Ribonucleoproteins

Index

List of figures

CHAPTER I

Introduction

1.1. Influenza A Virus

1.1.1. Influenza

The influenza A virus (IAV) is a significant cause of mortality around the globe, being responsible for some of the worst epidemics and pandemics in human history[1]. According to a report published online by the World Health Organization (2018), these yearly epidemics are estimated to provoke around 3 to 5 million cases of serious illness and 290 000 to 650 000 annual deaths[2].

There are three types of Influenza: A, B and C[3]. While types A and B are responsible for most cases of influenza infections, type C is not very clinically relevant and, among the first two, the majority of infections are induced by the IAV[3].

According to the International Committee on Taxonomy of Viruses (2018), the IAV species belongs to the Alphainfluenzavirus genus which is part of the Orthomyxoviridae family, and is classified as a type V virus according to the Baltimore classification system[4]. In the Orthomyxoviridae family, viruses are enveloped and have segmented, negative-sense single-stranded RNA genomes (ssRNA)[1,5]. IAV is additionally subdivided into multiple subtypes according to the conformation of its two most important envelope glycoproteins: hemagglutinin (HA) and neuraminidase (NA)[1,5]. Up until now, 18 types of HA (H1 to H18) and 11 types of NA (N1 to N11) have been discovered and identified[1,5–7].

Such as all viruses, IAV is an obligate intracellular parasite, taking control of the host cell's machinery in order to multiply and produce new viral particles[8].

1.1.2. Epidemiology and Disease

According to a World Health Organization report (2018), pandemic and epidemic influenza can affect all age groups, although some groups are more susceptible to developing serious illness than others such as the elderly, pregnant women, young children, individuals with chronic medical conditions, individuals with immunosuppressive disorders and health care workers. Seasonal influenza is an acute respiratory disease characterized by, among others, fever, cough, headaches and body aches[5,6], symptoms which usually appear after an incubation period of approximately 48 hours[6]. In most cases, when an individual contracts seasonal influenza, he/she can recover completely without resorting to treatment, except if that individual belongs to a risk group, in which case the disease can lead to severe complications, such as laryngotracheitis, haemorrhagic bronchitis and pneumonia[5,6]. Influenza can be transmitted by infectious droplets[6,9], aerosols[10–12] or physical contact[6,9].

The occurrence of a new influenza epidemic is due to the fact that influenza viruses are continuously undergoing antigenic evolution, either by antigenic shift or antigenic drift[6]. Antigenic drift is a continuous process, occurring in both influenza A and B, that is characterized by the accumulation of point mutations in the hemagglutinin and neuraminidase genes during viral replication[6,13]. The main goal of these mutations is to limit or even prevent antibody binding[5,13], allowing the new influenza virus variants to evade previous exposure or vaccination[6]. Antigenic shift is a sporadic event, occurring in

much less frequency than antigenic drift, that happens among influenza A viruses and induces the development of a novel virus strain due to genetic reassortment from RNA segments originating from different viruses or strains[5,6,14]. In this scenario, a large majority of the population does not have pre-existing protection (immunity) against this new strain of IAV which allows the new viral strain to rapidly disseminate among humans, potentially leading to new pandemics[5,6].

The most effective way to fight influenza A virus induced diseases is through prevention of infection by vaccination with inactivated or live attenuated vaccines, and administration of antiviral drugs[5]. Of the aforementioned methods, the most effective for prevention and control of influenza infection is vaccination[6,15] and a study conducted by the Centre for Disease Control and Prevention[16] estimated that 2018's vaccine had an overall effectiveness of 47%[16]. However, vaccines don't provide lifetime protection against influenza, offering protection for only a few months. This is due to the IAV antigenic drift and consequent antigenic evolution, making once effective vaccines ineffective against new strains[5]. This constant evolution of the virus makes it necessary to constantly evaluate and reformulate current vaccines in order to keep up with the antigenic drift of circulating strains of influenza[15].

Antiviral drugs can have both therapeutic and prophylactic effects, but, to prevent disease, they must be administered continuously at times of high influenza activity[5]. Two main types of antiviral drugs are used for the treatment of influenza: Matrix 2 ion channel blockers and neuraminidase inhibitors[5]. Matrix 2 (M2) ion channel inhibitors, such as Amantadine and Rimantadine[5,17,18], like the name suggests, block the M2 ion channel and prevent the release of the viral ribonucleoproteins (RNP) for migration to the nucleus of the cell[17,18], and on the other hand neuraminidase inhibitors, such as Zanamivir and Oseltamivir[5,17], induce the aggregation of viral particles on the host cell surface preventing the release of newly formed virions[17].

1.1.3. Structure (Genome and Morphology)

The IAV, like previously mentioned, is an RNA virus of the Orthomyxoviridae family and has a segmented, negative-sense single-stranded RNA genome ((-) ssRNA). The IAV genome is 13 588 bases long[19] and consists of eight single stranded, negative sense viral RNA (vRNA) segments that encode for at least 12 different viral proteins that are key factors for an efficient viral replication and virion formation in host cells[1]. These eight segments, which range in size from 890 to 2341 bases, contain conserved noncoding regions, of varying lengths, at both 3′ and 5′ ends, partially complementary to each other, that form a promoter for vRNA replication and transcription, by the viral polymerase complex[1,20]. These segments form ribonucleoprotein complexes (vRNPs) in conjunction with the viral RNA dependent RNA polymerase (vRdRp) complex, which consists of three different polymerase viral proteins, basic polymerase 1 (PB1), basic polymerase 2 (PB2), and acidic polymerase (PA)[1]. Each segment is separately encapsulated in the virion, by nucleoproteins (NPs), and arranged in a helical conformation to form the vRNPs[1] (Figure 1). Along the structure of the vRNPs, these virally encoded RNA-binding proteins (NPs) act as a helical scaffold, promoting tidily storage of the viral genome[1,21].

Out of the eight existing segments, the three largest encode the three viral proteins that assemble the vRdRp complex: PB1, PB2 and PA[22]. The three intermediate segments encode NPs and the membrane glycoproteins HA and NA[22]. Of the two remaining segments, the largest of them encodes the matrix protein M1 and the ion channel protein M2[22]. On the other hand, the smaller segment encodes two non-structural proteins, non-structural protein 1 (NS1) and non-structural protein 2/nuclear export protein (NS2/NEP)[22].

The viral genome is covered by an envelope (Figure 1) which consists of a lipid bilayer that is derived from the cellular membrane of the host cell during the budding process. The envelope is covered with the membrane glycoproteins HA and NA, and a small number of M2 proteins that go across the lipid envelope[1,20]. The type I transmembrane protein HA is the most abundant envelope protein at an approximate 80% presence in the virion envelope, followed by type II transmembrane protein NA, which makes up around 17% of the viral envelope proteins, which means that HA outnumbers NA in a ratio of approximately four to one[23]. When compared to the other two transmembrane proteins, M2, a type III transmembrane protein, is a very minor component of the viral envelope, with only 16 to 20 molecules per virion[23]. The lipid envelope and its three major proteins, HA, NA and M2 cover a layer of M1 proteins, that envelop the viral core and bind to the lipid envelope to maintain virus morphology[1]. The virion core, enclosed inside the M1 matrix, consists of the vRNP complexes which, like previously mentioned, comprise of viral RNA segments associated with viral nucleoproteins and the vRdRp complex (Figure 1). Inside the M1 matrix, besides the vRNP complexes, we can also find NEP/NS2, although their exact location in the virion structure is unknown[1,20].

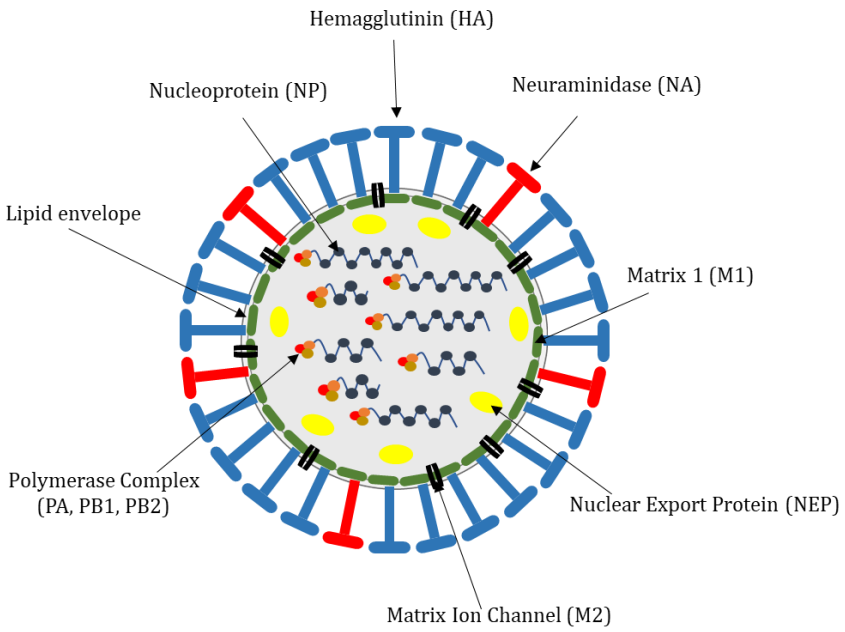

Figure 1. Schematic representation of the influenza A virus structure. IAV is an enveloped negative-sense single stranded RNA virus with a genome comprising of eight RNA segments encapsulated inside the virus particle.

IAV virions themselves, they usually present a spherical or elliptical shape but can also have filamentous forms which can exceed 300 nm in length[20]. Besides the most common forms, the virions can also present irregular shapes. The usual diameter of the virions can range from 80 to 120 nm and they can have varying lengths[1]. Despite all these varying characteristics, the core structure and components of the influenza virions remain the same, consisting of the same envelope containing its three integral transmembrane proteins and the eight vRNP complexes[1,20] (Figure 1).

1.1.4. Replication Cycle

The IAV is an obligate intracellular parasite, being completely dependent on the host cell machinery to replicate and propagate. The IAV life-cycle can be divided into the following phases: virus attachment, virus entry onto the host cell and release of viral content, nuclear transport onto the host cell nucleus, transcription and replication of the viral genome (synthesis of vRNA), export of the vRNPs from the nucleus and translation/synthesis of viral proteins and virus budding, and release from the host cell[20,23].

Virus Attachment: Upon entry onto a new environment, viruses circulate randomly until they end up clashing with the host cells. The IAV recognizes sialic acids on the host cell surface and, at that point, the IAV replication cycle initiates[20,23] (Figure 2, step 1). More specifically, the HA glycoprotein on the viral lipid envelope/membrane mediates the binding to sialic acid residues from glycolipids that reside on the surface of the host cells[6]. The specificity of HA's receptor binding is dependent on the nature of the glycosidic linkage between the sialic acid and the penultimate galactose residue on the receptor[20,23]. In human IAV strains, the termination of the HAs contains the sialic acid receptor binding site which is going to bind to sialic acids attached to galactose through a α(2,6) linkage, while in the case of avian IAV strains, viruses bind to sialic acids attached to galactose via an α(2,3) linkage[20,23].

Virus entry onto the host cell and uncoating: After a bond is established between the viral HA and the sialic acid residues on the surface of the host cell, the virus is internalized by receptor-mediated endocytosis[20,23]. Upon entry into the cell, the virus is involved by an endosome with an acidic nature (Figure 2, step 2). The low pH of the endosome (around 5 or 6) induces a conformational change in the HA glycoprotein of the virus envelope, exposing the HA2 fusion peptide (HA is made up of subunits: HA1, which contains the receptor binding domain, and HA2, which contains the fusion peptide[23]) triggering contact between the viral envelope and the endosome, which in turn leads to the fusion of the viral envelope with the endosomal membrane, and the creation of a "channel" (pore) through which the vRNPs are going to be released into the cytoplasm of the host cell[20,23]. Besides the fusion of the endosome with the viral envelope, the M2 ion channels, a transmembrane proton-selective ion channel that transverses the viral envelope, also open up, allowing a flow of hydrogen ions from the endosome into the viral core, acidifying it even more, weakening the interaction between the vRNPs and the M1 protein and causing their dissociation, which leads to the release of the vRNPs to the host cell cytoplasm[20,23].

Nuclear Transport: Once the vRNPs have been released from the viral structure, they are transported to the nucleus where they will undergo transcription and replication. This process (transport) occurs due to the viral proteins' (PA, PB1, PB2 and NP)[23] nuclear localization signals (NLSs), which induce the activation of the cellular nuclear import machinery by binding to the cellular nuclear import factor, importin alpha[24], to import the vRNPs into the host cell nucleus, through the nuclear pore complex[20,23,24] (Figure 2, step 3).

Synthesis of vRNA (Transcription and Replication of the viral genome): After the vRNPs are imported into the cell nucleus, synthesis of both the capped polyadenylated messenger RNA (mRNA), which is going to act as a template for host cell translation of viral proteins, and new vRNA strands, that are going to form the vRNPs of the new viruses, takes place[20] (Figure 2, step 4). Given that the IAV doesn't innately have the necessary components to carry out transcription independently, it hijacks the transcription machinery of the host cells.

Firstly, given that the RNA strands that make up the viral genome are negative sense, in order for them to be transcribed they must first be converted into positive sense RNA strands that are going to serve as a template for the production of new vRNA[20,23]. The vRdRp complex that was imported alongside the negative sense RNA segments plays an extremely important role in this process. The complex uses the vRNA as a template to produce two types of positive sense RNA: a full length uncapped and non-polyadenylated complementary RNA (cRNA), by replication, which is going to function as a model from which the RNA polymerase is going to transcribe more copies of negative sense vRNA, and mRNA, produced by transcription, which is going to serve as a template for viral protein synthesis[20].

The synthesis of the viral capped polyadenylated mRNA is initiated by a process called cap-snatching[23,25,26]. In this process, the viral polymerase uses the PB2 subunit of the vRdRp complex to promote the binding of the complex to short capped oligomers, located at the ends of the precursors of host mRNAs (pre-mRNAs)[25,26]. After binding, the viral polymerase uses its endonuclease domain in the PA subunit to cleave the pre-mRNAs at the 5' end, at a position 10–13 nucleotides downstream from the 5' cap[25,26]. The capped RNA fragment that is produced during this process, is going to be used by the vRdRp complex, via the catalytic PB1 subunit, as a primer to initiate viral mRNA synthesis, which eventually leads to the production of capped translatable viral mRNAs[25,26]. In contrast, the production of cRNA, by replication, does not require a primer to initiate[23,25].

Like previously mentioned, besides the vRdRp complex proteins, NP also expresses NLS and is imported into the nucleus, however the precise role that NP plays in viral RNA transcription and replication is not clear. Turrell et al., 2013[27] showed that the NP of IAV does not regulate the initiation or termination of either transcription or replication but instead, it supports the progress of the polymerase during the elongation phase[27].

Nuclear export and synthesis of viral proteins (Translation): Once mRNA is capped and polyadenylated, it can be exported out of the nucleus and translated by the host cell translation machinery[20].

Regarding the viral core proteins (PB1, PB2, PA, NP, NS1 and NS2/NEP), the virus hijacks and utilizes the host cell translation machinery for its own benefit, promoting translation of the viral mRNAs in the cytoplasm, in cytosolic ribosomes[20,26]. After being synthesized, in order to assemble the progeny vRNPs in the nucleus, the subunits of the vRNP complex (PB1, PB2, PA and NP) are imported from the cytoplasm back into the nucleus via their NLSs[28]. The PB1 and PA subunits can only be efficiently imported back into the nucleus after forming a dimer in the cytoplasm, while the PB2 subunit is imported separately and may undergo a conformational change on importin binding that promotes its binding to the PB1-PA dimer[28,29].

The viral envelope proteins HA, NA and M2, are synthesized in the endoplasmic reticulum (ER) membrane-associated ribosomes and are subsequently processed and folded in the ER and then trafficked to the Golgi apparatus where they undergo post-translational modifications, such as glycosylation[20,26] (Figure 2, step 5). These three envelope proteins possess apical sorting signals[20] that direct them through the trans-Golgi network to the host cell plasma membrane for subsequent virion assembly[20].

Assembly and nuclear export of vRNPs: After the import of vRdRp subunits (PB1, PB2 and PA) and NP back into the nucleus, vRNP formation occurs. The new vRNA segments that were synthesized by replication are encapsulated, co-transcriptionally, by a viral polymerase and free NP to form vRNPs[26,29].

The progeny vRNPs are exported from the nucleus into the cytoplasm by the cellular nuclear export factor CRM1/exportin1-mediated pathway and then transported to the cellular membrane[24], where virus assembly and budding takes place (Figure 2, step 6).

Virus packaging, assembly, budding and release: Assembly and budding of new influenza virions is a complex, multistep process that happens in a cholesterol rich membrane region, called lipid raft domain, on the apical membrane of infected host cells[30] (Figure 2, step 7).

It was previously thought that vRNA segments were randomly incorporated into budding viral particles, and only those particles that somehow ended up with a complete set containing all of the eight segments would become complete infectious viruses[20], however recent studies have shed a new light on this particular topic, suggesting that the viral packaging is a highly selective process in which discrete packaging signals present in all vRNA segments guarantee that the majority of progeny virions contain a complete genome with all eight segments[20].

After all the vRNP complexes and viral proteins are present near the cell membrane, budding occurs. Once that process is complete, the virus isn't immediately released because the HA is bound to the sialic acid residues from cell surface glycoproteins and glycolipids, retaining the virus until the NA, which is

anchored to the viral envelope by its transmembrane domain, cleaves those terminal sialic acid residues, due to its receptor destroying activity, and triggers the release of newly formed virions from the host cell[20,30] (Figure 2, step 7). The newly released mature virions are free to roam and spread the infection to other healthy cells in the respiratory tract.

While using the host cell to replicate itself, the virus causes the degradation and disruption of the cell, inducing the destruction of its membrane which eventually leads to cell death[31,32].

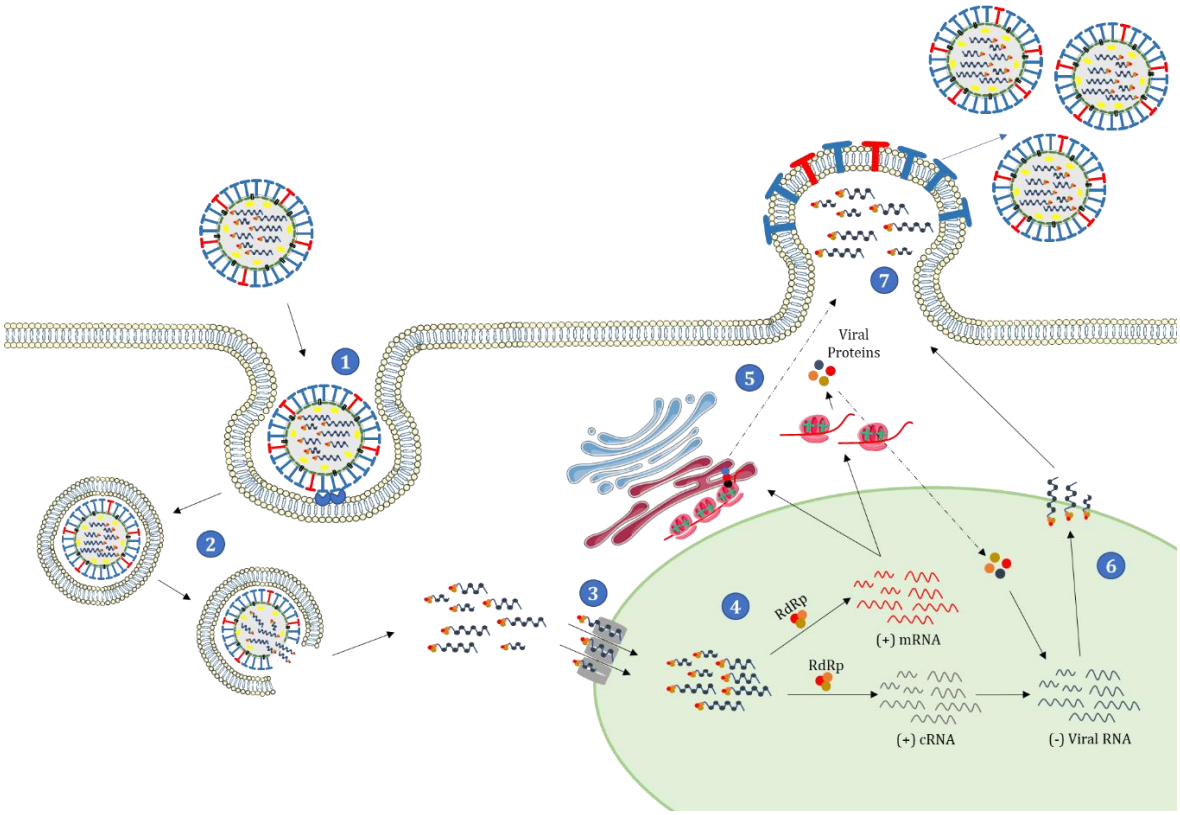

Figure 2. IAV replication cycle. The IAV hemagglutinin recognizes sialic acids on the host cell surface and, initiating, the IAV replication cycle initiates (1). The virus is then internalized via receptor-mediated endocytosis, and upon entry into the cell, the low pH of the endosome induces viral uncoating and the release of the viral genome into the cytoplasm (2). Transport of the genome to the nucleus occurs due to the viral proteins' (PA, PB1, PB2 and NP) NLSs, which induce the activation of the cellular nuclear import machinery (3). Upon entry onto the cell nucleus, viral genome undergoes transcription and replication (4). Synthesized mRNA is exported to the cytoplasm where viral core protein production occurs in the cytoplasm while viral envelope proteins synthesis and processing occurs in the ER and Golgi apparatus (5). Viral core proteins are imported back into the nucleus where vRNP production happens, while viral envelope proteins are transported to the host cell plasma membrane for subsequent virion assembly. Viral RNP complexes are formed in the nucleus, exported to the cytoplasm and transported to the cellular membrane (6). Assembly and budding of new influenza then occurs at the host membrane, followed by virion release (7). Adapted from Das et al., 2010[22].

1.1.5. Host Defences against IAV and IAV Mechanisms of Evasion

Upon detection of the presence of the virus, the host immune system is activated and it tries to actively fend off and clear the viral infection.

Innate Immune System: The immune response begins with the innate immune system which provides the first line of defence against IAV infection. This initial response is rapid but nonspecific and it's made up of physical barriers, such as mucus and collectins, phagocytic cells, cytokines and interferons (IFNs), all of which try to prevent infection of respiratory epithelial cells[33,34]. The activation of this response occurs when the pathogen associated molecular patterns (PAMPs) of the IAV are detected by the host cells pathogen recognition receptors (PRRs), such as retinoic acid-inducible gene-I protein (RIG-I)[33–35] , toll-like receptor (TLR)[33–35] and the NOD-like receptor family pyrin domain-containing-protein-3 (NLRP3)[34,35]. After recognition of PAMPs, RIG-I activates and its caspase activation recruitment domains (CARDs) become exposed, and are modulated by dephosphorylation or ubiquitination by E3 ligases[33]. Following this, CARD-dependent association of RIG-I and mitochondrial antiviral signalling proteins (MAVS), activates downstream transduction signalling at the outer mitochondrial membrane, which in turn leads to the activation of transcription factors, such as interferon regulatory factor (IRF) 3 and 7, and nuclear factor kappa-light-chain-enhancer of activated B cells (NF-κB), causing the expression of type I IFNs and proinflammatory cytokines[33,35]. Regarding TLRs, TLR3 and TLR7 are expressed on the surface of endosomes and lysosomes, and exclusively recognize nucleic acid PAMPs derived from multiple viruses, such as IAVs[33–35]. TLR3 specifically recognizes double stranded RNA (dsRNA) in endosomes while TLR7 binds ssRNA, particularly in plasmacytoid dendritic cells. TLR3 interacts with the TIR-domain-containing adapter-inducing interferon-β (TRIF) inducing the activation of serine–threonine kinases IκKε (IKKε) and TANK-binding kinase 1 (TBK1), which in turn phosphorylate to regulate the expression of interferon-β (IFN-β)[33], while TLR7 recognizes the ssRNA of influenza virions that are taken up into the endosomes, which leads to the activation of downstream signalling of TLR7, activating NF-κB, which induces the expression of proinflammatory cytokines, or IRF7 which promotes the expression of IFNs[33,35]. Finally, NLRP3, which is part of the NLRP3 inflammasome, is activated upon IAV infection, leading to the expression of genes encoding for pro-interleukin (IL)-1β, pro-IL-18, and pro-caspase-1, and is also activated when there is M2 ion channel activity, which leads to the activation of this inflammasome, and subsequent cleavage of pro-IL-1β and pro-IL-18[33–35].

Like previously mentioned, respiratory tract epithelial cells are usually the first targets of IAV after it enters the human organism and because of that they have developed the ability to produce and release several molecules, such as proinflammatory cytokines, chemokines and type I IFNs[35], that initiate the innate immune response by recruiting several innate effector cells, such as myeloid cells (monocytes and neutrophils) and lymphoid cells (natural killer (NK) cells)[33,35]. Besides these cells, other innate immune cells migrate towards the site of infection, such as dendritic cells and macrophages.

Adaptive Immune System: After the immune response takes place, the second line of defence of the immune system takes over. The adaptive immune system comprises the humoral immunity, which

consists of virus-specific antibodies, and cellular immunity, which consists of T lymphocytes (CD4+ and CD8+ T cells)[34]. Upon the first encounter with the invading virus, the adaptive immune response occurs very slowly when compared to the innate response. However, after the dendritic cells present viral antigens to naive T cells and the formation of immunological memory occurs, the response becomes faster and stronger after a second encounter with the same pathogen[36]

Mechanisms of evasion of the immune response by IAV: IAV proteins have the ability to bind and inhibit multiple components of the innate immune system, in part due to the high mutation rate of the influenza viral genome, which leads to the formation of antigenically different IAV strains that are able to evade recognition by the existing immune systems[34]. One of the main mechanisms that IAV has developed to evade innate immunity is the utilization of their NS1 protein to limit the innate immune response. This non-structural protein can bind the viral RNA with its RNA binding domain[34] and mask it in order to avoid recognition by TLRs and RIG-I, thus limiting type I IFN production[34,36]. Besides this, IAV also utilizes antigenic drift and shift to evade adaptive immunity.

1.2. Transfer Ribonucleic Acids

1.2.1. tRNAs: Function and Biogenesis

Transfer RNAs (tRNAs) are a type of non-coding RNAs (ncRNAs), and are ubiquitous adaptor molecules that by complementary codon-anticodon base pairing, ensure the incorporation of the correct amino acids in the forming polypeptides[37]. These molecules are a crucial part of the translation machinery, linking the genetic code in the mRNAs with the amino acid sequence of proteins[38]. There is a wide array of different tRNAs, with each of them being attached to a particular amino acid and being able to recognize a specific codon or codons in mRNAs[39]. TRNAs are relatively short molecules ranging from 73 to 90 nucleotides in size[38], and their structure is made up of five key areas: the acceptor stem (which includes a Cytosine-Cytosine-Adenine (CCA) termination), the D-arm, the TΨC-arm, the variable loop and finally the anticodon arm[37,38]. These structures will be presented in more detail in a further subchapter.

tRNA formation/biogenesis can be divided into seven basic steps: synthesis of the initial transcript, removal of the 5' leader sequence, trimming of the 3' trailer sequence, addition of the CCA termination, splicing of existing introns, modification of multiple residues and nuclear export of the tRNAs into the cytoplasm where the translation process takes place[40]. Initially, tRNAs are transcribed in the nucleus, by RNA polymerase III[41] as precursor molecules, named pre-tRNAs, that have accessory sequences at their 5' and 3' ends, 5' leader and 3' trailer respectively, that are removed during the maturation process[42]. In eukaryotes, the 5' leader sequence is usually removed first followed by removal of the 3' trailer sequence[40,42]. This process occurs in the nucleus of cells, and the removal of the 5' leader sequence is catalysed by the RNAse P enzyme, whereas the cleavage and removal of the 3' trailer sequence is catalysed by the RNAse Z enzyme[40,42]. After the cleavage of these sequences, the CCA termination is then added post-transcriptionally onto the maturing tRNA by a CCA-adding enzyme, which is a 3'-specific CCA nucleotidyltransferase[40,42]. After these stages of tRNA biogenesis, splicing of existing introns takes place, and this process is divided into two main steps: firstly, endonucleases recognize conserved elements of the anticodon arm and excise the introns[40,42], and secondly, two tRNA halves (3' half and a 5' half) are generated, after endonuclease induced removal of introns, which are then bound together by a ligase in order to complete the splicing process[40,42]. After all these steps are done, the maturing tRNA molecules go through a significant amount of post-transcriptional modifications, and are then exported into the cytoplasm where they can be incorporated and participate in the translation machinery[40].

TRNAs can be either attached to an amino acid, in a charged state or not attached to an amino acid, in an uncharged state[39]. An uncharged tRNA can be charged with an amino acid by an aminoacyl-tRNA synthetase[38], through an acyl linkage between the carboxyl group of the amino acid and the 3'-hydroxyl group of the adenine nucleotide at the end of the CCA termination at the 3' end of the tRNA[38,39]. This aminoacylation process can be divided into two main steps: adenylylation and tRNA charging[39,43], and the global reactions go as follows[43]:

(I) Amino Acid + ATP → aminoacyl-AMP + Pyrophosphate

(II) aminoacyl-AMP + tRNA → aminoacyl-tRNA + AMP

In the adenylylation step (I), the amino acid, which is bound to the synthetase, reacts with adenosine triphosphate (ATP) to become adenylylated, which means that the amino acid becomes associated with the phosphoryl group of adenosine monophosphate (AMP), and this is accompanied by the release of pyrophosphate (PP)[39,43]. Following adenylylation, tRNA charging takes place (II), in which the adenylylated amino acid reacts with the tRNA, inducing translocation of the amino acid to the 3' end of the tRNA, forming an aminoacyl-tRNA (aa-tRNA), with the release of AMP[39,43].

The newly formed aminoacyl-tRNA, which is a complex which comprises an amino acid associated with a tRNA, then participates in the peptide bond formation in protein synthesis[38].

Lastly, regarding their functions, tRNAs play other roles, though minor in comparison to their extremely important role in protein synthesis, such as the role of signalling molecules in the regulation of multiple metabolic and cellular processes[38], and formation of tRNA fragments (tRFs)[38]. Furthermore. aminoacylated tRNAs have been associated with cell envelope remodelling, antibiotic synthesis and protein labelling for degradation[38], among others.

1.2.2. tRNA Structure

The tRNA structure can be divided into its primary, secondary and tertiary structure[39,44]. The primary structure of tRNAs refers to the nucleotide sequence that constitutes the entire tRNA molecule, while the secondary structure, commonly referred to as cloverleaf since its shape resembles a four leaf clover, refers to the fundamental layout of the tRNA molecule, which folds into the tertiary, L-shaped, structure which represents the three dimensional shape of the tRNA molecule[39,44].

As mentioned, tRNAs are made up of four main substructures, which represent the four arms of the cloverleaf-like structure: the acceptor stem (which includes the 3' end CCA termination, which is the amino acid attachment site), the dihydrouridine (D) arm, the T pseudouridine (ψ) arm, and the anticodon arm[39,44] (Figure 3). Besides these four main substructures, the tRNA molecule also includes a small sized variable loop[37,39] (Figure 3). The four stems are short double helices stabilized by Watson-Crick base pairing[45], and upon folding the acceptor stem and the T-arm form a twelve base pair acceptor–TψC minihelix and the anticodon and D arms form another minihelix[44]. These two helices are positioned in a perpendicular fashion, putting the D-arm and T-arm into close proximity by non-canonical pairing of conserved nucleotides[44,46], while the anticodon arm and the acceptor stem are positioned on opposite ends of the tertiary structure of the tRNA molecule[44,46].

Acceptor stem: this substructure of the tRNA molecule is a double stranded stem formed by base pairing between the bases in the 3' and 5' ends of tRNA, and it includes the Cytosine-Cytosine-Adenine (CCA) termination which is the place where the bond between tRNA and amino acid, induced by aminoacyl tRNA synthetases, is established[39,45,47].

D-arm: this substructure is a double stranded stem of the tRNA molecule with a single stranded loop in its end, and it is believed to act as a recognition site for specific enzymes[48], however its exact role is still not yet fully understood. This loop contains dihydrouridine, a pyrimidine nucleoside which, according to the PubChem database of the National Center for Biotechnology Information, is the result of adding two hydrogen atoms to a uridine, hence the name "D-arm". This particular substructure of the tRNA is also believed to play an important role in the stabilization of the tertiary structure of the tRNA molecule and tRNA aminoacylation[49].

TψC-arm: just like the D-arm and the acceptor stem, the TψC-arm is also a double stranded stem with a single stranded loop in its end, and it is named this way due to the presence of thymidine, pseudouridine, which is a modified uridine nucleotide, and cytidine residues[39,44]. The stem is a five base pair motif frequently found in the structure of non-coding RNAs[50], and the pseudouridine base is often found within the 5'-TψUCG-3' sequence[39]. The T-arm is believed to play an important role in the stabilization of the tertiary RNA structure by facilitating long-range interactions between different regions of the molecule[50], and it is also involved in the facilitation of intermolecular RNA-RNA and RNA-ligand interactions in naturally-occurring molecules[50].

Variable loop: this loop, as its name implies, varies in size ranging from 3 to 21 bases long, and is located between the anticodon arm and the TψC arm[39]. The canonical and most common tRNA molecule is usually around 73 to 76 bases long and any additional bases are usually included by the variable loop, hence its variable size[44].

Anticodon Arm: much like the previous substructures, the anticodon arm contains a double stranded stem with a single stranded loop in its end, which contains an anticodon[39]. Anticodons are, almost always, boxed between a purine, on the 3' end, and an uracil residue, on the 5' end[39], and are units made up of three nucleotides that match to the three bases of the codon in the template mRNA[39,44]. After recognition of one another, the first and second bases of the mRNA codon interact with the second and third bases of the tRNA anticodon by Watson-Crick base pairing[39,45] (Adenine – Uracil or vice-versa and Guanine - Cytosine or vice-versa), however the interaction between the third base of the codon and the first base of the anticodon is more flexible, since it allows non-Watson–Crick base pairing[39,45]. This particular position of the tRNA molecule (position 34 of the tRNA structure), was then named the wobble position[39,45,51–53]. Like mentioned, this location of the tRNA molecule supports non-standard base pairing, such as a Guanine - Uracil pairing, which in terms of length and structure is quite similar to the standard Guanine - Cytosine base pair[45]. This feature allows tRNAs the ability to pair with more than one codon, and furthermore, allows multiple codons to code for a single amino acid[52,54]. This particular feature of the genetic code is called degeneracy of the genetic code[55]. Of the 64 existing codons, 61 represent amino acids and 3 represent stop signals, which means that 61 types of tRNA molecules would be necessary to cover all codons[55]. However, this isn't the case because the genetic code is described as degenerate, which means that although each codon is specific for only one amino acid, a single amino acid may be coded by more than one codon[55].

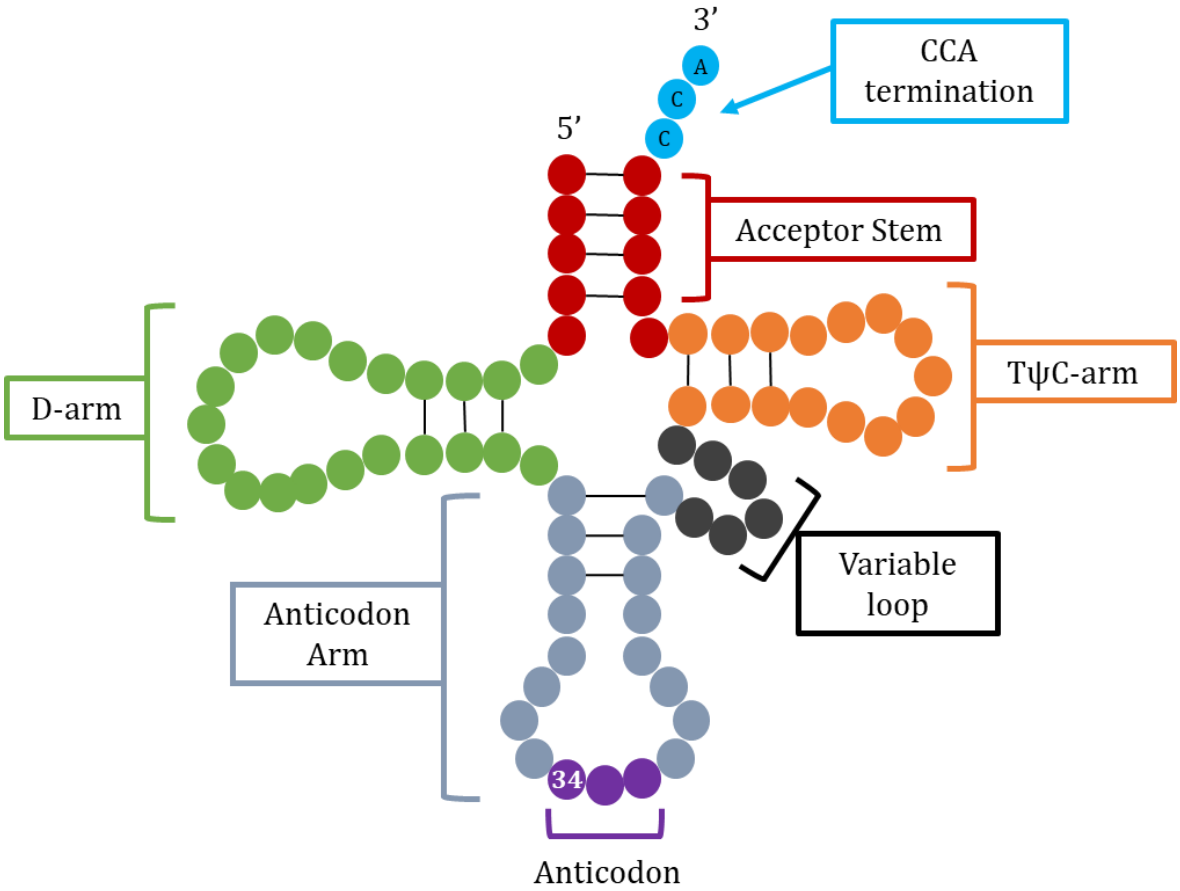

Figure 3. Schematic representation of the tRNA secondary structure. Transfer RNAs are made up of four main substructures, which represent the four arms of the cloverleaf-like structure: the acceptor stem (which includes the 3' end CCA termination), D-arm (which includes the stem and the loop), the TψC -arm, and the anticodon arm. Besides these four main substructures, a small sized variable loop can also be found between the anticodon stem and TψC stem. Connecting lines between residues indicate base pairing. Adapted from Pereira et al., 2018[54].

1.2.3. tRNA Modifications

As approached previously, tRNA biogenesis starts off with the synthesis of the initial transcript, followed by processing of the 5' and 3' ends of the pre-tRNAs, addition of the CCA termination, splicing of introns[40], and before being involved in protein synthesis and other processes, the tRNA molecule undergoes a great number of post-transcriptional modifications, which happen in multiple bases throughout the entire tRNA structure, to ensure tRNA stability, and translation accuracy and efficiency[37,53,54,56–58]. All of these modifications that happen throughout the tRNA molecule are catalysed by different tRNA-modifying enzymes (TMEs)[54,57].

These modifications are not exclusive to human/mammal tRNAs, and are a common feature of tRNAs from all organisms[40], however eukaryotic tRNAs tend to be more heavily modified than bacterial tRNAs, while parasitic and plastid tRNAs tend to be the least modified[59]. According to a report by MODOMICS,

a database of RNA modification pathways[60], 163 post-transcriptional modifications of RNA have been identified, of which at least 80 of them are found in tRNAs[60,61]. On average, a tRNA molecule has 13 modifications[62], and the main goal of them is to introduce a functional diversity that allows the four basic nucleotide residues to obtain new functions[60]. Among all functions that are induced by post-transcriptional modifications, some can be highlighted, such as promotion of functional folding and tRNA stability by modifications occurring at the TψC and D arms[54,59], stabilization of codon-anticodon interaction by modifications at position 37 near the anticodon loop[54,61] and correct codon-anticodon base pairing, and reading frame maintenance by modifications occurring in the anticodon, more specifically, at position 34, also known as the wobble position[54,61,63]. Among the modification spectrum, some modifications are relatively common to all tRNAs, such as dihydrouridine, in the D- arm, which is the result of the reduction of the carbon-carbon double bond at positions 5 and 6 of the uridine base by dihydrouridine synthases[64], pseudouridine, in the TψC arm, which is the result of a non-reversible isomerization of uridine (pseudouridylation) catalysed by pseudouridine synthases[65], the N6-isopentenyl modification to adenosine (i6A) modification at position 37 of tRNAs, or the methylation of uridine to 5-methyluridine at position 54 of the in the TψC arm[66], while other modifications are specific to certain tRNAs or groups of tRNAs[44,54], such as the modification of guanosine to wyosine at position 37 of $tRNA^{Phe}$ of eukaryotes[66].

Modifications can range from simple additions or substitutions of functional groups, such as methyl, amine, and thiol groups, to large complex structures, whose biosynthesis depends on the interaction between multiple components of different pathways[37]. Even though multiple bases throughout the tRNA molecule are modified, the anticodon is particularly subjected to a wide variety of modifications, more specifically at the wobble position[40,52]. Like mentioned, these modifications potentiate the increase in tRNA capacity to decode multiple synonymous mRNA codons, which differ between themselves in the third nucleoside, and also enhance recognition by the aminoacyl-tRNA synthetase enzymes, and serve as a preventive measure against frame shifting during the translocation process[52]. Some of the most common modifications of Uridine at the wobble position (U34) are the 5-methoxycarbonylmethyl (mcm^5) or the 5-carbamoylmethyl (ncm^5) modifications catalysed by the elongator complex, which results in a modified uridine residue, named mcm^5U34[61]. Following this modification, U34 is usually further modified by a sulfur-relay pathway, which is catalysed by URM1, inducing thiolation (addition of a 2-thiol group) of U34 resulting in a 5-methoxycarbonylmethyl-2-thiouridine (mcm^5s^2U) nucleotide[61].

Like mentioned, the structural core of tRNAs is also heavily impacted by modifications. For example, methylations found at the tRNA core, which includes the TψC and D arms, are important for proper folding[59,66]. One example of this is the pseudouridine (ψ) modification, which is one of the most abundant base modifications, found at a variety of different positions in tRNAs[59]. In the TΨC-loop, it forms a tertiary base pair with a base in the D-loop contributing to the overall stability of the tertiary tRNA

structure[59]. Further ψ are distributed all over the entire tRNA structure, where they might also contribute to the overall stabilization of the tRNA molecule[59].

Due to certain stimuli or in certain conditions, deregulation of tRNA modifications may occur as a result of tRNA-modifying enzyme misexpression. As a result, tRNAs can be either hypo or hyper-modified, which ultimately may lead to compromised translation accuracy and fidelity, leading to serious changes in the normal functioning of the cell potentially developing into a disease[54].

1.2.4. tRNA-Modifying Enzymes

TRNA post-transcriptional modifications are catalysed by tRNA-modifying enzymes (TMEs). Until now, 100 TMEs have been identified[67], with organisms from the eukarya, archaea and bacteria domains reserving a significant fraction (3 to 11%)[68] of their genome to the coding of TMEs involved in the post-transcriptional modification of nucleosides in tRNAs[53,67]. Relatively recent studies have carried out transcriptome wide analysis of the translation process, via ribosome profiling, in order to get a better understanding of the role of TMEs in translation and proteostasis[69], and even though great progress has been made in this field, the role of many modifications and TMEs remains undiscovered and unidentified[69].

Multiple genetic mutations in TMEs have been associated with different pathological conditions, most notably, neurological and metabolic disorders, which indicates that irregular behaviour/functioning of TMEs leading to hypomodification of tRNAs, could be linked to the development of human diseases[54]. This data that has been collected over the years suggests that TMEs might be part of the set of molecules that are required for life[68].

Of the multiple existing TMEs, our work was focused on six particular enzymes: ELP1/IKBKAP, ELP3 and ELP6 of the elongator complex, TRMT2A, ALKBH8 and URM1 (Figure 4). The following paragraphs are going to give an overview over the type of modifications they induce.

Elongator Complex (ELP1, ELP3, ELP6): the elongator complex is a 6-subunit complex, highly conserved in eukaryotes, made up of two smaller subcomplexes: one containing ELP1, ELP2 and ELP3 and another one containing ELP4, ELP5 and ELP6[40,70]. This complex has been described as a component of a hyperphosphorylated RNA polymerase II holoenzyme[71], and has also been characterized as a complex that induces acetylation of histones H3 and H4[72], and that regulates exocytosis due to the interaction between ELP1 and Sec2, an essential Rab GTPase[40,71,72]. Initially, this complex was thought to be a transcriptional elongation complex of RNA polymerase II in the nucleus, hence its name, with no other remarkable function, however it was later discovered that it is primarily a cytoplasmic complex that promotes translation fidelity and efficiency by inducing one of the first post-transcriptional modifications in the wobble position: the addition of a 5-methoxycarbonylmethyl (mcm^5) or 5-carbamoylmethyl (ncm^5) group to the U34[40,61]. Of the subunits composing the complex, ELP3 is of particular interest given that it has been described as the catalytic subunit of the elongator complex[61,73].

The reason for the interest in this particular subunit stems from the fact that multiple studies have shown that this TME is involved in the development of some disorders, more specifically, it has been associated with Wnt-driven intestinal tumor initiation[74] and its deletion in cortical stem cells initiates the untranslated protein response (UPR) impairing the formation of intermediate neuronal progenitors eventually leading to the development of microcephaly[61,75]. ELP3 has also been described as a modifier/risk factor for amyotrophic lateral sclerosis (ALS)[76,77]. ELP3 mutations promoted abnormal synaptic development, possibly leading to neurodegeneration, which implies that this enzyme plays an important role in axonal biology and can be identified as a gene which might lead to neuronal degeneration[77].

URM1: the ubiquitin-related modifier 1 protein, commonly known as URM1, is a ubiquitously expressed protein, and a member of the ubiquitin superfamily[78,79]. Analysis of this superfamily has shown that URM1 has the most conserved structural and sequence characteristics of the common ancestor in the entire ubiquitin superfamily[80]. As previously mentioned, after the modifications induced by the elongator complex, U34 is usually further modified with a 2-thiol group (thiolation) by a sulfur-relay pathway, in which the URM1 enzyme acts as a sulfur carrier, resulting in a 5-methoxycarbonylmethyl-2-thiouridine (mcm^5s^2U) U34 nucleotide[61,78,79].

ALKBH8: AlkB Homolog 8, commonly called ALKBH8, is one of many AlkB homologues identified in humans[81,82]. This enzyme possesses a methyltransferase domain and it's involved in the last step of the formation of 5-methylcarboxymethyl uridine, by catalysing the methylation of 5-carboxymethyl uridine (cm^5U) to 5-methylcarboxymethyl uridine (mcm^5U) at the wobble position in the anticodon loop of tRNAs[81,82]. Besides this role in tRNA modification, ALKBH8 has also been implicated in bladder cancer progression by promoting angiogenesis and growth of these types of cancer[83].

TRMT2A: according to the "Gene" database of the National Centre for Biotechnology Information (NCBI), the tRNA methyltransferase 2 homolog A, also known as TRMT2A, is a protein often used as a biomarker for certain types of breast cancer[84], however it is also known for inducing tRNA modifications due to its RNA methyltransferase domain[85]. TRMT2A is a homolog of the yeast (*Saccharomyces cerevisiae*) TRM2p enzyme[86], and it catalyses a 5-methyluridine (m^5U) modification at position 54 of the tRNA molecule, located at the TψC arm, which is one of the most common modifications found in tRNAs[85].

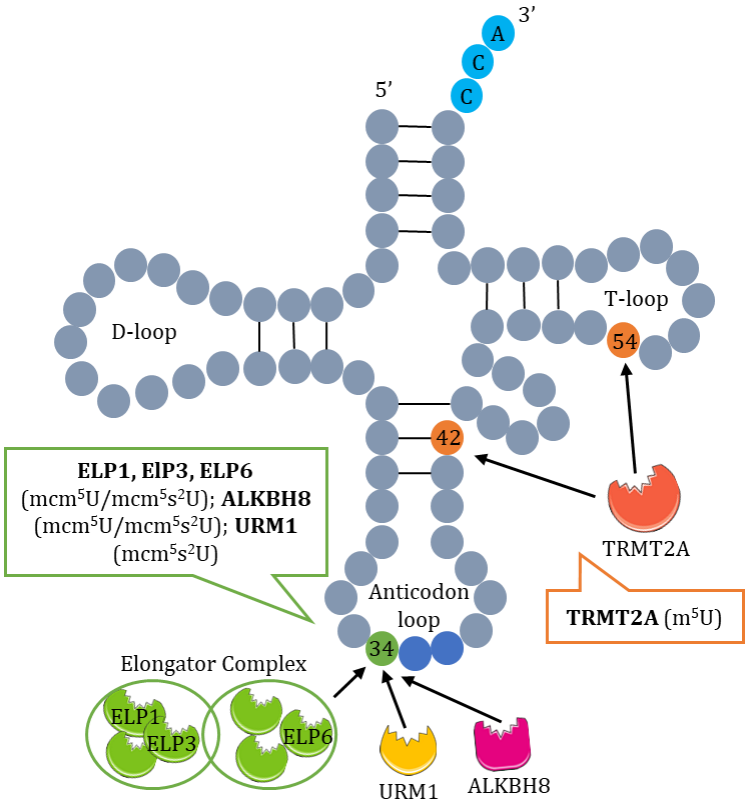

Figure 4. Transfer RNA secondary structure with the respective tRNA-modifying enzymes and modifications (in parenthesis). The elongator complex subunits ELP1, ELP3 and ELP6 act on the wobble position in the anticodon loop. Similarly, URM1 and ALKBH8 also act on this position of the tRNA structure, while TRTM2A induces modifications in the TψC loop. Adapted from Pereira et al., 2018[54].

1.2.5. Interaction between IAV and tRNAs

The majority of viruses are completely dependent on the host cell translation machinery to produce their own viral proteins. Because of this, viruses developed an array of mechanisms that allows them to manipulate the tRNA population to their own benefit with the ultimate goal of adjusting viral codon usage to the host cell tRNA pool in order to guarantee that translation occurs in the most efficient, seamless and error-free way possible[87]. As one would expect, the host codon usage matches and reflects the host tRNA population, so it is logical to believe that when viral codon usage is similar to that of the host, viral translation occurs in an efficient manner, however most of the time this isn't the case and viral codon usage usually seems poorly adapted to the hosts tRNA population[87,88].

One of the most common and well-known examples of tRNA pool manipulation is the case of HIV-1[89]. HIV-1 genes are expressed in a temporal manner (earlier in the infection the virus expresses an "early" set of genes and later in infection it expresses a "late" set of genes)[89]. The early genes are translated in the tRNA pool that normally translates highly expressed human genes[89], which ends up not being too advantageous to the virus, since its codon usage is poorly adapted to the tRNA population of the host[89]. However codon usage of HIV-1 late genes is significantly more adapted to the tRNA pool of the host,

which according to van Weringh et al., 2011[89], is altered and selectively enriched to favour HIV-1 codon usage, suggesting that HIV-1 induces alterations in the tRNA pool throughout infection[89].

Regarding IAV, Pavon-Eternod et al.[90] found that upon nuclear export of the capped and polyadenylated freshly produced viral mRNA to the cytoplasm, IAV interacts with the tRNA population of the host cell translation machinery[88,90]. Using microarray technology[90], the authors showed that, while the total tRNA population remained more or less unchanged upon IAV infection, the polysome-associated tRNA population changed substantially in a virus-specific way, showcasing that the virus altered and optimized the hosts' tRNA population to better match IAV codon usage[90]. Furthermore, the authors suggested the possibility of the existence of localized tRNA pools at sites of viral translation in the cytoplasm, which would include specifically recruited tRNAs that decode codons rare in the host but common in the virus[90]. These pools would be tailored to viral codon usage, to enhance translation efficiency of IAV genes[90].

Although literature and research around this particular topic (interaction between IAV and tRNAs) is relatively scarce, these results demonstrate that IAV is indeed able to manipulate the tRNA pool of the infected cells[88,90].

On the context of interaction between viruses and TMEs, literature is also rather limited. There is, however, one example involving Mimivirus[91]. This virus encodes a homolog of the tRNA (uracil-5-)-methyltransferase, the tRNA-modifying enzyme whose Escherichia coli counterpart catalyses the methylation of uracil at position 54[91].

In my work, I dove deeper into this subject and studied the interaction between IAV and the TMEs that extensively modify tRNAs post-transcriptionally, in order to determine whether IAV infection induces changes in the expression of TMEs and if that is a mechanism by which viruses modulate the tRNA pool to favour viral protein translation.

CHAPTER II

Aims of the Study

Influenza A Virus infection impact on the pool of TMEs of the host

Even though tRNAs are absolutely vital to the correct functioning of the cell, we are still only at the verge of uncovering the exact mechanisms by which tRNAs interact with other components of the translation machinery, as well as the complex functions mediated by post-transcriptional tRNA modifications.

Many studies have been made around the topic of tRNA modifications and TME deregulation and the development of diseases[92], more specifically neurological[77,93,94] and metabolic disorders[95,96], and cancer[97,98]. These studies have showcased that hypomodified tRNAs and low activity of TMEs are often associated with neurodegenerative diseases[76,99], while hypermodified tRNAs and high activity of TMEs are associated with the development of cancer[97,98].

In the context of viruses and viral infections, most of the research has been focused on the way the viruses interact with the tRNAs and not the TMEs that modify them. Due to the high medical relevance of IAV and the previous results obtained concerning the regulation of tRNAs by IAV, we were interested in studying the interplay between IAV infection and tRNA modifications and TMEs.

In this study, we set out to determine whether IAV infection leads to changes in the TME pool of host cells. More specifically we wanted to determine whether IAV induced alterations in the expression of some key TMEs (ELP1, ELP3, ELP6, URM1, ALKBH8 and TRMT2A), upon infection, and whether manipulating the levels of TMEs prior to infection would lead to alterations in viral propagation.

CHAPTER III

Materials and Methods

3.1. Materials

3.1.1. Cell lines

A549	Adenocarcinomic human alveolar basal epithelial cells
MDCK	Madin-Darby Canine Kidney cells
HeLa	Human cervix adenocarcinoma cells; stable cell line that is expressing the fluorescent reporter HSP27-GFP. Multiple variations of this cell line were used besides the wild type variation: ELP3 Knockout HeLa cells and Control/Scramble HeLa cells
HEK293T	Human cell line, derived from the HEK293 (Human embryonic kidney 293 cells) cell line, that expresses a mutated SV40 large T antigen

3.1.2. Viruses

Influenza A Virus (PR8)	Influenza A Virus (Strain A/Puerto Rico/8/1934 H1N1)

3.1.3. Cell Culture Stock Solutions

Dulbecco's Modified Eagle Medium (DMEM): High Glucose, with L-Glutamine and without Sodium Pyruvate, from Gibco™
Fetal Bovine Serum (FBS), qualified and E.U.-approved, from Gibco™
Penicillin/Streptomycin (P/S), from Gibco™
Dulbecco's Phosphate Buffered Saline (PBS), without Calcium and Magnesium, from BioWest
Trypsin-EDTA, without Calcium, Magnesium and Phenol Red, from Gibco™

3.1.4. Antibiotics

Puromycin (10 mg/mL), from Sigma-Aldrich

3.1.5. Markers and Loading Dyes

GRS Protein Marker Multicolour, from Grisp
6x Laemmli Buffer, containing DTT and Bromophenol Blue

3.1.6. Buffers and Prepared Solutions

BSA 1%	BSA 2% diluted in 1x PBS
PFA 4%	20 g PFA in 450 mL ddH_2O, 4 drops 1 M NaOH, 50 mL 10x PBS
0,2%Triton X-100	0.2% Triton X-100 in 1x PBS
Mounting Medium (Mowiol)	12 g Mowiol 4-88, 20 mL Glycerol, 40 mL PBS
DMEM +/+	DMEM supplemented with 50 mL of FBS and 5.5 mL of P/S
SFM	DMEM supplemented with 5 mL of P/S
1xPBS (Non-Cell Culture)	1.37 M NaCl, 80 mM NaHPO4, 0.0268 M KCl, 0.0147 M KH2PO4, pH = 7.3, prepared from 10x PBS diluted in ddH2O
Ethanol 100%	Pure ethanol
Ethanol 70%	70 mL of ethanol 70% and 30 mL of ddH_2O
MiliQ H_2O	RNAse free H_2O
ELB	0.5% Triton X-100, 50mM Hepes pH = 7, 250mM NaCl, 1mM DTT, 1mM Naf, 2mM EDTA, 1µM EGTA, 1mM Na3VO4 in ddH2O Before use, add inhibitors: 0.01 mM Foy, 0.25 (v/v) Trasylol, 0.1 mM PMSF
BSA 7%	0.7 g of BSA in 10 mL of ddH_2O
TPCK Trypsin	0.001 g of TPCK Trypsin in 1 mL of MiliQ H_2O
Avicel Solution (2.4%)	2.4g of Avicel powder in 100 mL of MiliQ H_2O
10x Acid Wash Buffer	1.35 M NaCl, 0.1 M KCl, 0.4 M Citric Acid, pH = 3 in 20 mL of ddH_2O
1x Acid Wash Buffer	1.35 M NaCl, 0.1 M KCl, 0.4 M Citric Acid, pH = 3, diluted in 180 mL of ddH_2O

0.1% Toluidine Blue in PFA 4%	0.05 g of Toluidine Blue in 50 mL PFA 4%
Chloroform	
Milk for Blot blocking	5 g of milk powder 100 mL of 1x TBS-T
1xTBS-T	100 mM Tris Base, 150 mM sodium chloride and 0.05% Tween-20, pH = 8
1xRunning Buffer	250 mM Tris, 1.9 M Glycine and 1% SDS
2-mercaptoethanol (β-Mercaptoethanol)	
Loading buffer	1 M Tris (pH = 6.80), 10% Glycerol, 1 M DTT, 20% SDS, β-Mercaptoethanol, 0,1% Bromophenol Blue

3.1.7. Antibodies

3.1.7.1. Primary antibodies

		Dilution		
Antibody	**Species**	**IMF**	**WB**	**Supplier**
NP	Rabbit	1:1000	1:1000	IGC
NS1	Rabbit	-	1:500	IGC
HA	Mouse	-	1:1000	Santa Cruz
FK2	Mouse	1:300	-	Ana Raquel Soares
ELP3	Rabbit	-	1:200	Ana Raquel Soares

3.1.7.2. Secondary antibodies

		Dilution		
Antibody	**Species**	**IMF**	**WB**	**Supplier**
Alexa 488	Rabbit	1:500	-	Invitrogen

Alexa 647	Mouse	1:500	-	
TRITC (561)	Rabbit	1:100	-	Jackson Imunoresearch
	Mouse	1:100	-	Jackson Imunoresearch
Anti-Mouse 680	Mouse	-	1:1000	
Anti-Rabbit 800	Rabbit	-	1:1000	
DAPI	-	1:2000	-	

3.1.8. Kits

Pierce™ Bovine Serum Albumin (BCA) Protein Assay Kit, from Thermo Scientific
Protran BA85 Nitrocellulose Blotting Membrane, from GE Healthcare
High-Capacity RNA-to-cDNA™ Kit, from Applied Biosystems™
NZY Total RNA Isolation Kit, from Nzytech
mirVana™ miRNA Isolation Kit, from Life Technologies™

3.1.9. Reverse Transcriptase-Quantitative Polymerase Chain Reaction (RT-qPCR) Master Mix and probes

Mastermix	
TaqMan™ Gene Expression Master Mix	Applied Biosystems (by Thermo Fisher Scientific)

Probes	
ELP1	TaqMan ® Gene expression Assays from Applied Biosystems (by Thermo Fisher Scientific)
ELP3	TaqMan ® Gene expression Assays from Applied Biosystems (by Thermo Fisher Scientific)
ELP6	TaqMan ® Gene expression Assays from Applied Biosystems (by Thermo Fisher Scientific)

URM1	TaqMan ® Gene expression Assays from Applied Biosystems (by Thermo Fisher Scientific)
ALKBH8	TaqMan ® Gene expression Assays from Applied Biosystems (by Thermo Fisher Scientific)
TRMT2A	TaqMan ® Gene expression Assays from Applied Biosystems (by Thermo Fisher Scientific)

3.1.10. Software and Databases

Excel 2016, Microsoft
REST 2009, M. Pfaffl (Technical University Munich) and QIAGEN
7500 Software, Applied Biosystems
DeNovix DS-11 Software, DeNovix
ZEN Software, Zeiss
Image Studio Software for Odyssey
Prism 8, GraphPad
ImageJ, Fiji
National Center for Biotechnology Information (NCBI)
Google Scholar, Google

3.2. Methods

3.2.1. Cell Culture (Subculture)

After thawing frozen cell stocks, cells were kept at 37°C, 5% CO_2 with complete DMEM (DMEM (Gibco®) supplemented with 10% FBS and 1% Pen-Strep). Cell line maintenance was performed every week. Cells were cultured and split twice a week in 100 x 20 mm cell culture dishes with complete medium.

After the cells reached high confluency (70-80%) they were washed with PBS and incubated with 2 mL of Trypsin at 37°C, 5% CO_2 for approximately 5 minutes. After being separated, lifted and detached from the dish surface, cells were resuspended in complete DMEM and prepared according to experimental needs and/or seeded in a 1:10 dilution.

The HeLa cells utilized in this project were maintained in cell culture with medium containing puromycin in a concentration of 2 µg/ml. Medium was changed every 48 to 72 hours.

3.2.2. Cell storage, freezing and thawing

Cell stocks were prepared from cells in culture with high confluency (around 90%). After being trypsinized for 5 minutes, cells were collected, to a falcon, with complete medium followed by centrifugation. The cell pellet was resuspended in freezing medium (DMEM supplemented with 10% Dimethyl Sulfoxide (DMSO) and 10% FBS). Finally, cells were kept in cryovial aliquots of 1 mL, which were then frozen at -80ºC before being stored in a liquid nitrogen tank for cryopreservation.

When needed, frozen cells were resuspended in culture medium, at room temperature, and seeded in 100 x 20 mm cell culture dishes. Cells were then kept at 37ºC, 5% CO_2 to grow. Following cell adhesion, the medium was replaced by fresh medium to remove cell debris and DMSO.

3.2.3. Cell Seeding

When needed to perform experiments, cells were washed with PBS and trypsinized at 37ºC, 5% CO_2 for 5 minutes, centrifuged at 1000 rpm for 3 minutes and then resuspended in 10 mL of complete DMEM. Cell count was done through a Neubauer Chamber. The number of cells needed varied depending on the cell line that was being used. Finally, 1 to 3 mL of cells were seeded, and the plates were incubated at 37ºC, 5% CO_2 for approximately 24h.

3.2.4. Infection

General protocol of infection

To perform an infection with Influenza A virus PR8, A549 or HeLa cells were seeded the day prior to the infection.

When cell seeding is done, an extra well is prepared which is going to be used to count the cells ahead of the infection, in order to prepare an appropriate virus dilution (it's important to have in consideration the MOI (Multiplicity Of Infection) that we want to use (MOI = 3) and the pfu/ml of the virus (1,7 x 10^7 pfu/ml and 2,08 x 10^7 pfu/ml (two different values of pfu/ml because new virus aliquots were produced while conducting the experiments))). Firstly, we aspirated the medium in which cells were incubated with, and wash them with PBS or Serum Free Media (DMEM supplemented with 1% P/S) to remove the FBS from the complete medium, since FBS can inhibit virus entry into cells. After removing the PBS or SFM we infect the cells with IAV PR8, at a MOI of 3, diluted in SFM (750 µL per well) while control cells were mock-infected with 750 µL of SFM and were referred to as Mock throughout the experiments. Afterwards we put the plates on the rocker for 15 minutes at room temperature to induce virus entry, followed by a 45 minute incubation at 37ºC, 5% CO_2, after which we add DMEM supplemented with 20% FBS and 1% P/S, to block the entry of new viruses into the cells, (we must add the same volume of it (750 µL in this case), to have FBS at a final concentration of 10%) and subsequently we incubate (37ºC,

5% CO_2) for the times wanted (2 hours, 4 hours, 6 hours and 8 hours for the Reverse Transcriptase-Quantitative Polymerase Chain Reaction (RT-qPCR) experiments and 16 hours for the plaque assay experiments).

Infected samples harvesting

For the plaque assay experiments, cells are incubated with BSA 7% in SFM, instead of DMEM supplemented with 20% FBS and 1% P/S to allow the cells to grow and for newly produced viruses to leave the cell.

In the several desired timepoints we harvested the respective samples: coverslips for immunofluorescence, cell pellets to process with the mirVANA and NZYTech RNA isolation kits or the Pierce™ BCA Protein Assay Kit, and supernatants for the plaque assay experiments. For the plaque assay experiments we collected the supernatants, which were stored at -80ºC, while for the RT-qPCR experiments, wells were washed with PBS and coverslips were transferred to new 12-well plates where they were incubated with 4% PFA for 20 minutes at room temperature. The coverslips were then stored at 4ºC. Cells were then trypsinized for 5 minutes at 37ºC, 5% CO_2, collected to 1,5 mL eppendorfs and centrifuged for 3 minutes at 3000 rpm. Following centrifugation, the supernatants were discarded leaving only the pellets which were then stored at -30ºC for posterior RNA extraction/isolation.

3.2.5. Immunofluorescence

To perform Immunofluorescence, we used A549 or HeLa cells that grew in 12 mm glass coverslips. Cells were washed twice with 1x PBS and then fixated with 4% PFA for 20 minutes at room temperature. Afterwards, the coverslips were washed three times with 1x PBS and cells were permeabilized with 0,2% Triton X-100 for 10 minutes at room temperature. Subsequently, coverslips were once again washed three times with 1x PBS and blocked with 1% BSA for 10 minutes at room temperature. After washing three times with 1x PBS, specific targets were stained with 20 µL of primary antibody for 1 hour (followed by three washes with 1x PBS) and 20 µL of secondary antibody also for 1 hour (followed by three more washes with 1x PBS) protected from light. Incubation with DAPI was also done (20 µL of DAPI for 3 minutes at room temperature). Lastly, the coverslips were dipped in dH_20, and mounted in glass slides with a drop of Mowiol (mounting medium) and dried for at least 24h. The slides were then stored at 4ºC until observation under a microscope.

3.2.6. RNA extraction/isolation

Using the pellets that were obtained after infection and stored at -30ºC we performed RNA extraction using the NZYTech (NZYTech - Genes & Enzymes) and mirVANA (Introvigen™ by Thermo Fisher Scientific) RNA isolation kits.

NZYTech's NZY Total RNA Isolation kit: Kit was utilized according to the manufacturer's instructions. Firstly, we added buffer NR and β-mercaptoethanol to the cell pellets and vortexed vigorously to induce cell lysis. After that we applied the lysate into an NZYSpin Homogenization column placed into a 2 mL collection tube, centrifuged for 1 minute at 11,000 g and saved the flow-through. After that we added 70% ethanol to the flow-through and mixed immediately by pipetting up and down to purify the RNA. Then, we pipetted the lysate onto an NZYSpin Binding column, centrifuged at 11,000 g for 30 seconds, discarded the flow-through and placed the column into a new collection tube. After that we added Buffer NI and centrifuged at 11,000 g for 30 seconds, discarded the flow-through once again and placed the column back into the same collection tube. Subsequently for each isolation, we applied digestion mix (to digest the DNA) directly into the center of the silica membrane of the NZYSpin Binding column and incubated at room temperature for around 15 minutes. Then, we added NWR1 buffer (washing buffer) and centrifuged for 1 minute at 11,000 g, discarded the flow-through and placed the column in a new collection tube. We then added Buffer NWR2 (washing buffer), and centrifuged at 11,000 g for 1 minute, discarded the flow-through and placed the column back into the same collection tube. We repeated the wash with Buffer NWR2 and centrifuged, once again, at 11,000 g for 2 minutes to dry the column membrane and then discarded the flow-through. Finally, we placed the NZYSpin Binding Column in a clean RNase-free microcentrifuge tube, added 30 μL of RNase-free water directly to the column membrane and centrifuged at 11,000 g for 1 minute to elute the RNA. We then stored the RNA at -30ºC for further use (cDNA synthesis). All the buffers, mixes and columns utilized during this protocol were included in the RNA Isolation Kit sold by NZYTech (with the exception of 70% Ethanol and β-mercaptoethanol).

mirVana™'s miRNA Isolation Kit: Kit was utilized according to the manufacturer's instructions. We started by adding Lysis/Binding Solution and vortexed vigorously to completely lyse the cells and to obtain a homogenous lysate. After that we added miRNA Homogenate Additive to the lysate and mixed well by vortexing, and then we left the mixture on ice for 10 minutes. Following that, we added Acid-Phenol:Chloroform and vortexed for 60 seconds to mix. Then we centrifuged the samples for 10 minutes at 10,000 g, at room temperature, to separate the aqueous and organic phases. Subsequently we carefully removed the aqueous/upper phase, and transferred it to a new tube (every time we did this process, we took note of the volume that was transferred). We then added 1,25x volume of room temperature 100% ethanol to the aqueous phase (1,25 times the volume that was transferred to a new tube) and, for each sample, we placed a Filter Cartridge into one of the collection tubes supplied and subsequently pipetted the lysate/ethanol mix onto that Filter Cartridge. After that we centrifuged the tubes with the filter cartridges for approximately 15 seconds at 10,000 g and discarded the flow-through. Finally, we performed the washing steps by applying the miRNA Wash Solution 1 to the Filter Cartridge and centrifuged for 10 seconds and then discarded the flow-through. Ten, we applied Wash Solution 2/3 and centrifuged once again. We then repeated this step and, after discarding the flow-through from the last wash, we transferred the Filter Cartridge into a fresh collection tube, applied MiliQ water and spinned for 30 seconds at maximum speed to recover the RNA. To finalize, we collected the

eluate and stored it at -30ºC for cDNA synthesis. All the buffers, solutions and filters utilized during this protocol were included in the mirVana's Isolation Kit (with the exception of 100% Ethanol, Chloroform and MiliQ water).

The RNA that was obtained was then quantified using DeNovix DS-11 spectrophotometer (Nanodrop).

3.2.7. RNA Quantification

As mentioned, after RNA isolation using both kits (mirVana and NZYTech), we then quantified the obtained RNA. Firstly, we defined "Blank" using RNAse free water and after that we quantified the RNA (maximum absorbance at 260 nm) in each of the 8 samples that we obtained (Mock 2,4,6,8h and PR8 2,4,6,8h). The spectrophotometer that was utilized measures, simultaneously, the absorbance at 230, 260 and 280 nm, which allows it to determine the A260/A230 and A260/A280 ratios, which can indicate if there are traces of contamination in our samples. The A260/A230 ratio usually indicates if there is contamination by organic compounds and the A260/A280 ratio indicates if there is contamination by protein specimens. A A260/A280 ratio of 2.0 and a A260/A230 ratio of 1.8 to 2.2 are generally accepted as an indication that the extracted RNA is pure.

3.2.8. cDNA synthesis

Using the RNA that was obtained after RNA extraction and stored at -30ºC, we synthetized cDNA using the Applied Biosystems™ High-Capacity RNA-to-cDNA™ Kit. To synthetize RNA using this kit we need the RNA obtained from the RNA isolation, RNAse free water and both solutions included in the kit (RT Buffer Mix and RT Enzyme Mix). According to the manufacturer's product information sheet, the total volume per reaction was 20 µl. Per reaction we utilized 500 ng of RNA, which filled up to 9 µl with RNAse free water, 10 µl of RT Buffer Mix and 1 µl of RT Enzyme Mix. Samples were incubated at 37ºC for 60 minutes, followed by a 5 minute incubation at 95ºC to stop the reaction, and finally held at 4ºC (Figure

5). This reaction was performed in a Thermocycler (MyCyler by BioRad). The cDNA that was obtained was stored at -30ºC for further use (RT-qPCR).

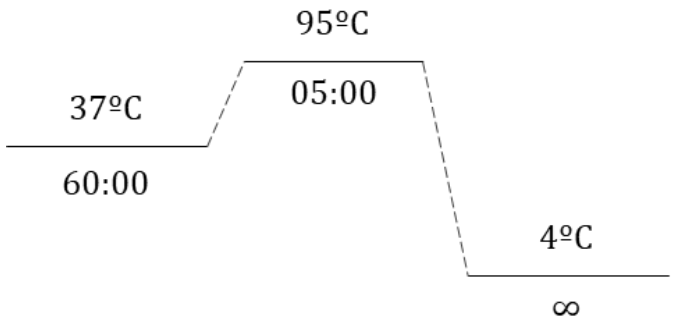

Figure 5. Cycling protocol for cDNA synthesis. Samples were incubated for 37°C for 60 minutes. Reaction was stopped by heating the samples to 95°C for 5 minutes and held at 4°C. This protocol was run in a thermocycler.

3.2.9. Reverse Transcription-Quantitative Polymerase Chain Reaction

Using the cDNA that was obtained, we performed a wide array of RT-qPCRs. We used the TaqMan™ Gene Expression Master Mix and followed the user guide instructions. We prepared reaction mixes for each of the samples/conditions that we wanted to test. Each condition/sample was done in triplicate to increase the accuracy and fidelity of our results, and each reaction had a volume of 20 µl multiplied by four so that each eppendorf had 80 µl (60 µl divided by three wells (20 µl in each well) plus 20 extra µl to guarantee that we had enough). Thus, each reaction mix contained 10 µl of TaqMan™ Gene Expression Master Mix, 1 µl of the cDNA templates that we prepared, 8 µl of RNAse free water and 1 µl of the TaqMan® Gene Expression Assays that we wanted to test (ELP1, ELP3, ELP6, URM1, ALKBH8, TRMT2A and GAPDH as a housekeeping gene to normalize our results). After vortexing, 20 µl of reaction mix was added to each well of a standard optical 96-well reaction plate and then the reaction plate was covered with an adhesive sealing film. The plate was then centrifuged for 3 minutes at 800 rpm. The reaction was measured using the cycling protocol described in figure 6 in the 7500 Software. The fluorescence was measured after the annealing/extension step using the previously mentioned software (7500 Software).

After the cycling protocol was finished, the data was exported to an excel file and analysis of gene expression data was performed using the REST 2009 Software.

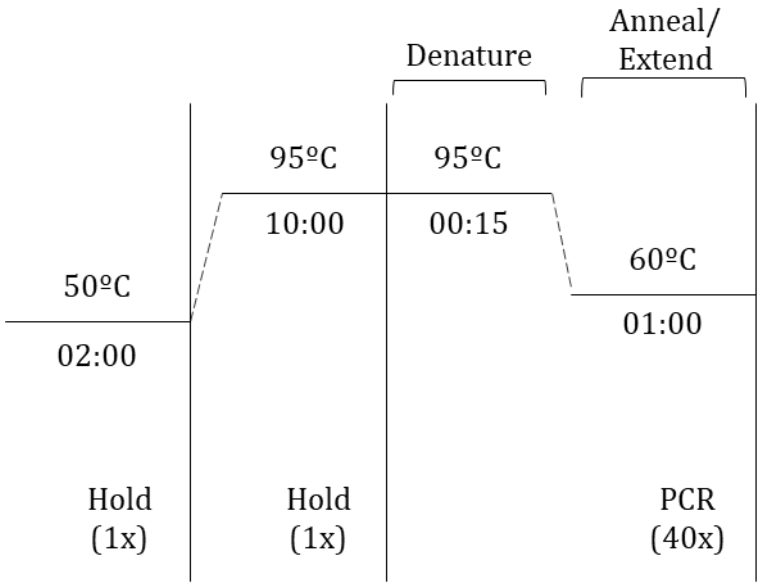

Figure 6. Cycling protocol used to amplify the tested genes. The PCR cycle started with uracil-N-glycosylase (UNG) incubation for optimal activity (50ºC for 2 minutes) followed by polymerase activation at 95ºC for 10 minutes and 40 cycles of a denaturation-annealing-extension step.

3.2.10. Plaque Assay

Using the supernatants that were collected upon infection, we performed plaque assays. Plaque assays are used to determine viral titre as plaque forming units per milliliter (pfu/ml). To start the experiment, we seeded a large amount of MDCK cells (6 x 10^5 cells per well in 12-well plates) and let them grow for 24h in complete medium to form a cell monolayer, which were then infected with the supernatants collected, using serial dilutions, to have a low amount of virus, so that only sporadic cells become infected. When a cell gets infected, the produced viruses immediately infect adjacent cells, that eventually lysate and induce the formation of what is called a "plaque", remaining surrounded by uninfected cells. The individual plaques obtained from successive dilutions can be counted to calculate the virus titre (pfu/ml).

One day after seeding MDCK cells, we defrosted the viral supernatants (collected from the infected and mock cells) and vortexed them. We prepared serial dilutions from 10^{-1} to 10^{-5} (55 µl of each supernatant were added to 500 µl of SFM, vortexed, and 55 µl of that solution was subsequently diluted). After aspirating the medium from the MDCK wells, cells were rinsed with 1 ml of PBS, before being infected with 300 µl of the prepared dilutions from -1 to -5 (for the non-infected (mock) cells only the -1 dilution was considered). After infection, we left the plates for 10 minutes on the rocker followed by an incubation of 45 minutes at 37ºC and 5% CO_2. After incubation, we added 1 ml of an avicel solution to each well (2.4% Avicel, SFM, 0.14% BSA and 1:1000 TPCK Trypsin) and we put the plates back into the

incubator for approximately one and a half days. After this long incubation, we removed the solution, rinsed the wells with PBS and added toluidine blue in 4% PFA, and left the plates on the rocker overnight. Finally, we removed the toluidine blue in 4% PFA solution, washed the wells with tap water and let the wells dry. After the wells were dried up, we counted the plaques in each dilution and performed the necessary calculations.

3.2.11. Immunoblotting

Total Protein Extraction

After infection cell pellets were collected and stored at -30ºC for protein extraction. Cells were resuspended with 100 µl of Empigen Lysis Buffer (ELB) supplemented with inhibitors (0.01 mM Foy, 0.25 (v/v) Trasylol and 0.1 mM PMSF). After resuspension with ELB, cells were sonicated twice for 15 seconds (this process induces the disruption of cell membranes in order to release the cellular contents). After sonication, samples were centrifuged for 20 minutes at 200 g and 4ºC. Supernatants were then collected (pellets were discarded) and stored at -30ºC until quantification. Throughout the whole process, samples were kept on ice to avoid the activity of proteases. Protein quantification was performed as described below in the next point (3.2.12.).

Protein Sodium Dodecyl Sulfate-Polyacrylamide Gel Electrophoresis (SDS-PAGE)

After quantifying the protein in each sample, we could then determine the desired volume of protein extracts to use for Western Blot. The desired amount of protein for each sample was diluted in 6x loading buffer (1 M DTT and 0.1% bromophenol blue) and denatured at 95ºC for 5 minutes, and samples were loaded onto polyacrylamide gels that were previously prepared. The resolving gel varied from 10 to 12% polyacrylamide and the stacking gel was 4% polyacrylamide. Besides the multiple samples, a pre-stained protein marker (GRS Protein Marker Multicolour Grisp) was also loaded onto the gel. After mounting the system and loading the marker and the samples, the electrophoretic chamber was filled with 1x running buffer until the majority of the glass was covered. Firstly, the electrophoresis was run at 80V for, approximately, 30 minutes to allow the samples to pass through the stacking gel and then at 120V for 90 minutes.

Western Blot

After the electrophoresis run was finished, we transferred the proteins from the gel onto a nitrocellulose membrane using the Trans-Blot® Turbo™ Transfer System at 25V for 30 minutes. After transfer, membranes were washed three times, 5 minutes each, with 1x tris-saline buffer with Tween 20 (TBS-T) to remove residues that remained in the membrane. After washing, the membranes were blocked with 5% powder milk diluted in TBS-T for 1 hour at room temperature. After blocking, membranes were stained through incubation with primary antibodies in a mixing plate/rocker overnight at 4ºC. The day

after, membranes were washed three times, 5 minutes each, with 1x TBS-T and incubated with the respective secondary antibodies for one hour in a mixing plate/rocker, at room temperature protected from light. Membranes were washed, once again, three times, 5 minutes each, with 1x TBS-T. Revealing of the stained membranes was done using the Odyssey Imaging System and the obtained images were analysed using its associated software. This system possesses two infrared channels (700 and 800) for fluorescence.

3.2.12. Protein Quantitation Assay

In order to quantify the total protein in each sample, Pierce™ Bovine Serum Albumin (BCA) Protein Assay Kit was utilized following the manufacturer's instructions included in their user guide. Total extracts with the BCA reagent were incubated for 30 minutes at 37°C followed by absorbance measurement at 575 nm using a microplate reader. Resulting data was then exported in excel format.

3.2.13. Viral Production

HEK293T cells were seeded ($5x10^5$ cells in a 6-well plate). The day after, cells were transfected with the correspondent segments to produce either PR8 and dNS1 (a type of IAV which lacks the NS1 protein).

For PR8 production, eight segments (PB2, PB1, PA, HA, NP, NA, M and NS1) were cotransfected, while for dNS1 production, the last segment was substituted by a shorter sequence to produce a truncated protein. The transfection was performed by mixing 0.25 µg of each segment's plasmid with polyethylenimine (PEI) reagent (1 µg DNA: 8 µl PEI) in 200 µl SFM and, after vortexing and a 15 minute incubation at room temperature, each mix was added to the correspondent cells dropwise, and cells were incubated overnight at 37°C and 5% CO_2. The day after, the medium was changed to 2 mL of SFM with 0.14% BSA and 1 µg/ml Trypsin-TPCK. After two days of incubation under the same conditions, the supernatant was collected and subjected to centrifugation at 3000 rpm for 5 minutes. Clarified supernatant with low amount of viruses (P0) were stored at -80C until further procedures.

To produce viruses with workable titre (P1), $6x10^6$ MDCK cells were seeded into a T75 flasks and put them in the incubator at 37°C and 5% CO_2 for 24 hours. After washing the cells twice with PBS, cells were infected with 200 µl of P0 aliquots in 5 ml of SFM supplemented with 0.14% BSA and 1 µg/ml Trypsin-TPCK, followed by a 15 minute incubation under agitation and 45 minutes at 37°C and 5% CO_2. Afterwards, 10 ml of the same media was added to the cells, that were let to grow for 48h under the same conditions.

At this point, supernatants were collected and centrifuged for 5 minutes at 3000 rpm. Clarified supernatants were then aliquoted and stored at -80°C. The pellets obtained after centrifugation can be

used to confirm the infection through western blot against viral proteins, more specifically NP and NS1. To titrate the viruses produced, we performed a plaque assay after one free-thaw cycle of P1 aliquots.

3.2.14. Statistical Analysis

Statistical analysis was done using Graph Pad Prism 8. Data was attained for the quantitative analysis of expression of TMEs (ELP1, ELP3, ELP6, URM1, ALKBH8 and TRMT2A) from at least three independent replicas/experiments and bars represent means with the standard deviation (SD). To determine the statistical significance between the experimental groups a two-way ANOVA followed by Bonferroni's test were applied. P values of ≤0.05 were considered as significant.

CHAPTER IV

Results and Discussion

4.1. Influenza A Virus infection impact on the pool of TMEs of the host

In order to determine whether IAV infection induces alterations in the pool of TMEs (Figure 7), we infected A549 cells with the PR8 virus, a wild type virus which is one of the most commonly used strains of IAV (A/Puerto Rico/8/1934 (H1N1)). Cell pellets for RNA isolation, and fixed cells for immunofluorescence were collected 2 hours post infection (hpi), 4 hpi, 6 hpi and 8 hpi. In all of these time points we not only collected the infected samples, but also mock/control samples for comparison. In this initial stage of the project only the wild type strain of IAV (PR8) was utilized.

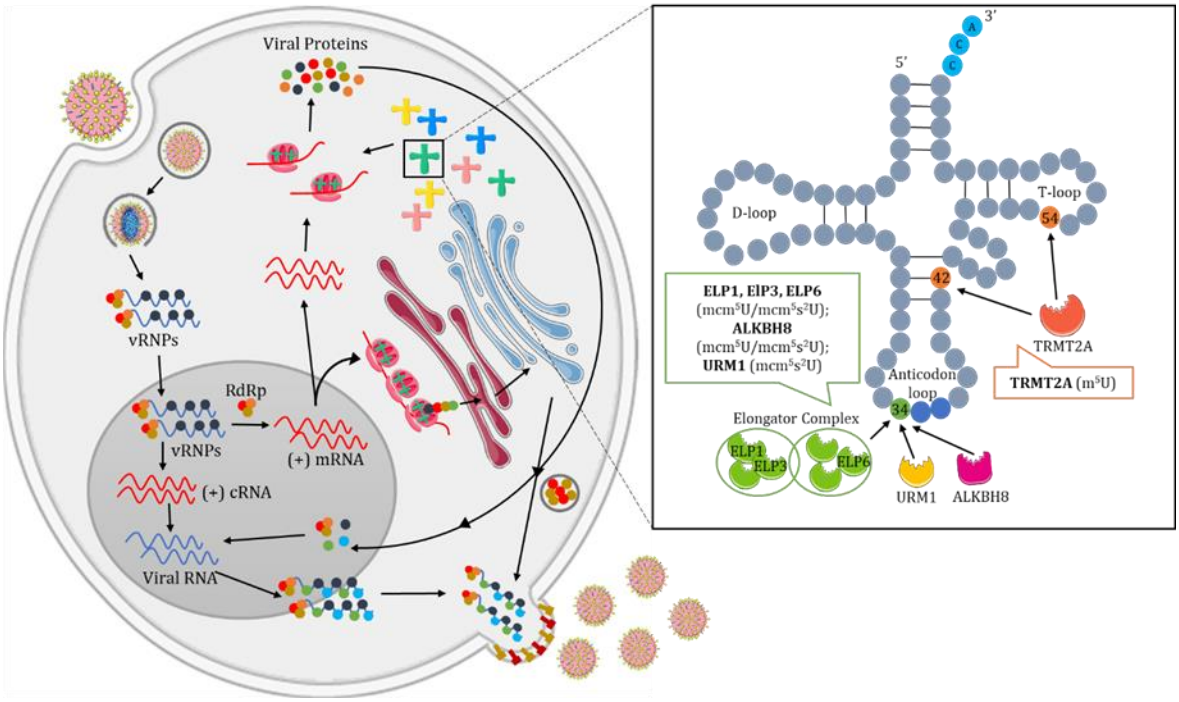

Figure 7. Schematic representation of IAV life-cycle and tRNA secondary cloverleaf structure. Upon infection of a living cell, IAV takes control of the host cell translation machinery to produce its own viral proteins. It has been shown that IAV interacts and induces changes in the tRNA population of the host cell. Our study is going to approach the potential interaction between these two entities.

Before we advanced in the procedure and extracted RNA from the multiple collected samples, we firstly confirmed whether IAV infection was successful. In order to do that we performed an immunofluorescence protocol in the fixed cells that were obtained upon infection, and stained them with an anti-NP primary antibody. Analysis by confocal microscopy indicated that infection was indeed successful, with the virus located in the expected cellular compartments in all time points (at 2 hpi the viral genome is still in the cytoplasm since the virus has just entered the cell, at 4 hpi the viral genome is already inside the nucleus. At 6 hpi some viral genome can be already be detected in the cytoplasm however the majority is still inside the nucleus, while at 8 hpi the virus genome has completely left the nucleus and newly formed viral particles are ready to leave the cell), and with mock/control cells not showing traces of viral infection (Figure 8).

After confirmation of infection, RNA of the collected samples was extracted/isolated using isolation kits. This was followed by complementary DNA (cDNA) synthesis, and subsequent run of RT-qPCRs. At least three biological replicas were performed, and six different TMEs were tested in this study (ELP1, ELP3, ELP6, URM1, ALKBH8 and TRMT2A).

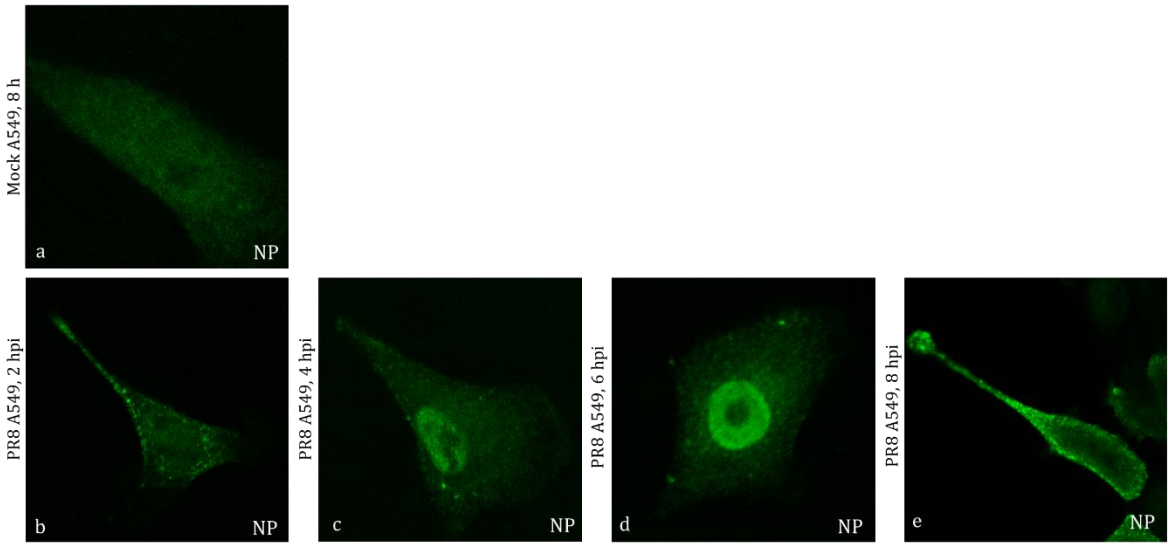

Figure 8. Successful viral infection in A549 cells infected with PR8 IAV. Confocal images from immunofluorescence staining of NP with anti-NP primary antibody. (a) A549 mock-infected cells 8h after incubation, (b) A549 infected cells 2 hpi, (c) 4 hpi, (d) 6 hpi and (e) 8 hpi; viral protein NP is shown in green.

Out of the multiple TMEs that catalyse changes in tRNAs, we decided to focus on these six, due to the rather important modifications they induce. The elongator complex is of great interest, given that it induces one of the first post-transcriptional modifications in the wobble position (mcm^5 or ncm^5), and without it a lot of other TMEs can't induce their modifications. However, instead of analysing the six subunits of the complex, we focused on ELP3, which is the catalytic subunit of the complex and one member of each of the two subcomplexes: ELP1 and ELP6. Besides these TMEs we also included ALKBH8, URM1 and TRMT2A in our study. ALKBH8 acts in the final biogenesis' step of mcm^5, due to its methyltransferase domain. URM1 is involved in the subsequent thiolation of the wobble position, resulting in a mcm^5s^2U nucleotide. Finally, TRMT2A catalyses a m^5U modification at position 54 of the tRNA molecule, in the TψC arm, which is one of the most common modifications found in tRNAs.

ELP1, ELP3, ELP6, ALKBH8 and TRMT2A are overexpressed two hours post infection with IAV

RT-qPCR analysis of the expression levels of the genes coding for the tRNA-modifying enzymes ELP1, ELP3, ELP6, URM1, ALKBH8 and TRMT2A, at different time points upon infection with IAV, showed that ELP1, ELP3, ELP6, ALKBH8 and TRMT2A were overexpressed two hours after infection as opposed to URM1 which had normal expression levels in this time point (Figure 9). No other striking changes were detected in the remaining time points (4 hpi, 6 hpi and 8 hpi), given that the expression of the multiple TMEs was within the thresholds considered for normal expression (0.5 – 1.5). IAV(PR8)/Mock ratio was calculated using the REST 2009 software and the expression values were normalized with GAPDH. TMEs with expression values below 0.5 were considered as underexpressed and above 1.5 were considered as overexpressed.

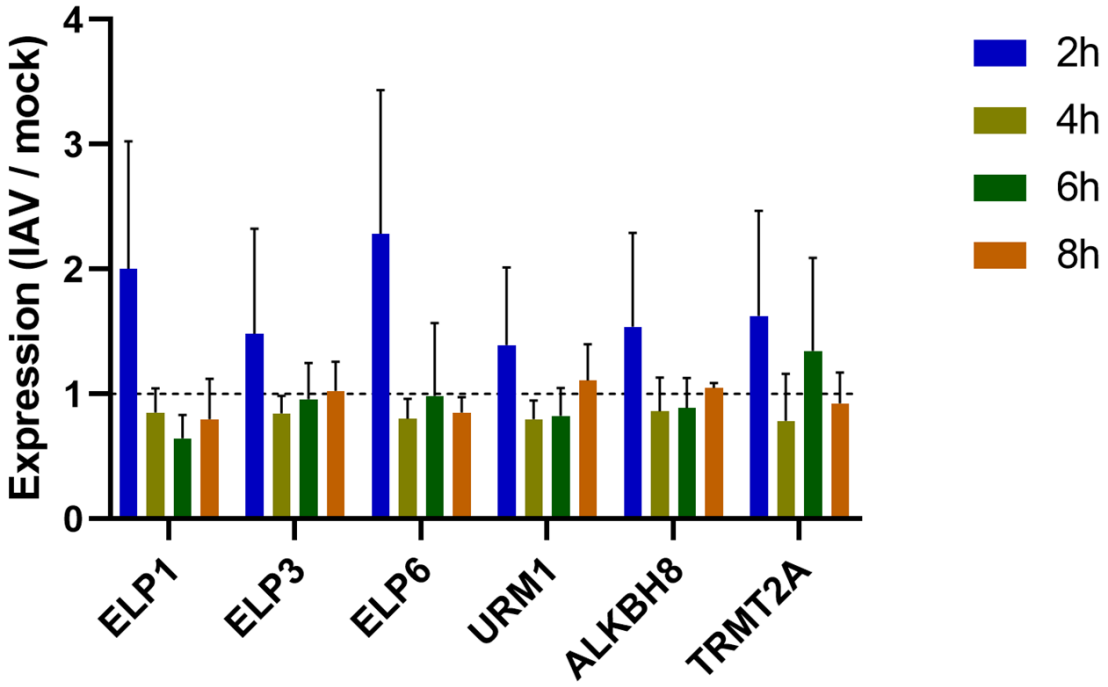

Figure 9. RT-qPCR analysis of the expression levels of tRNA-modifying enzymes (ELP1, ELP3, ELP6, URM1, ALKBH8 and TRMT2A) at different time points upon infection with IAV. Expression values (Infected cells (PR8) against Mock cells (SFM)) of six different TMEs in four distinct time points: 2 hours (when the virus entered the cell), 4 hours (when the virus is in the nucleus), 6 hours (after the viral genome has already started exiting the nucleus) and 8 hours (when the virus has mostly left the nucleus and is moving towards the plasma membrane). Expression values were normalized with GAPDH (expression values represented by the dotted line).

At 2 hpi, we obtained expression values of 2.0 for ELP1, 1.5 for ELP3, 2.3 for ELP6, 1.5 for ALKBH8 and 1.6 for TRMT2A, while URM1 presented a normal expression value of around 1.4. In the other time points (4 hpi, 6 hpi and 8 hpi) the multiple tested enzymes presented normal expression values, ranging from 0.5 to 1.5, as previously mentioned.

As mentioned, at 2 hpi the virus genome is still mostly located in the cytoplasm[100], while at 4 hpi the virus genome is already inside the nucleus where it undergoes replication and transcription. At 6 hpi, some viral NP can already be detected in the cytoplasm, and finally at 8 hpi the virus genome has completely exited the nucleus and virus particles are being formed at the cytoplasmic membrane, ready to leave the cell. After 6 hpi, is generally when viral protein production is thought to occur in the cytoplasm, using the host translation machinery, and that would, theoretically, be where the expression of TMEs would be affected, however that is not what we observed during our experiments. Throughout the multiple biological replicas, it was only at 2 hpi that overexpression of TMEs was detected, and since at this time point the virus genome still hasn't translocated into the nucleus this might indicate that, for some reason, cells increase the expression of these genes as a response to IAV infection or, on the other hand, it might indicate that IAV, upon entry onto the cell, induces overexpression of these modification enzymes, promoting a higher modification rate of cellular tRNAs in order to increase the number of mature/functional tRNAs available for the virus to utilize during the viral protein production phase of its life-cycle.

Literature regarding this particular area is thin, making it quite difficult to extrapolate the reason why the expression of TMEs is higher in this particular time point. One avenue of investigation that could be explored is the analysis of the expression of these TMEs using different strains of influenza, such as H5N1, other viruses with a life-cycle similar to IAV or even other completely different viruses, such as the HIV-1 virus, which is another RNA virus, to see whether these changes in the expression of genes coding for TMEs are strain or virus specific or if multiple different strains/viruses are affected in a similar fashion. HIV is one of the most researched viruses on the subject of interaction between viruses and tRNAs, mostly due to the fact that HIV-1 recruits human $tRNA^{Lys3}$ to serve as the reverse transcription primer via an interaction between lysyl-tRNA synthetase (LysRS) and the HIV-1 Gag polyprotein[89,101], which sparked great interest among researchers. Given that HIV-1 already has a track record of interacting with tRNAs, it could be interesting to observe whether it also induced changes in the expression of TMEs similar to those induced by IAV.

In our experiment, like previously mentioned, at least three biological replicas were performed in order to get a reliable and solid analysis, however even with this number of replicas we still observed some variance in our experiments, with some enzymes presenting a wide range of expression values, as happened with ELP1 and ELP6 which presented relatively large standard deviation (SD) values. Given that the entire experimental procedure is quite complex, involving many different protocols and a wide variety of different steps spawning multiple days, this can somewhat explain why in some cases a variance in the expression values can happen. One solution would be to perform a higher number of

replicas in order to get an even clearer picture of the expression profile of each enzyme, and maybe increase the number of time points earlier on in the infection to pinpoint when exactly does the peak of expression occurs. Another avenue we eventually plan on taking is to get a complete picture of the expression profile of most TMEs during infection. In order to achieve this, we plan on using a multi-well plate (upwards of 300 wells) which requires specific equipment to run and provides a wider read on other untested enzymes that may present expression changes at 2 hpi or even at other time points, which may be interesting targets for further research.

In summary, ELP1, ELP3, ELP6, ALKBH8 and TRMT2A appear to be overexpressed two hours after infection with IAV, while no changes were detected in other time points. Although, as mentioned, solidification of our results and further studies must be performed, namely to obtain the expression profile of other TMEs in the multiple time points, our results indicate that IAV interferes with the TME population of host cells.

4.2. Effect of the lack of a TME on IAV propagation

Following the first part of our study, we wanted to analyse the importance of TMEs in viral production to further understand the interplay between IAV and TMEs. In order to determine whether the lack of one of these TMEs, more specifically the ELP3, the catalytic subunit of the elongator complex, would influence viral particle production by the infected cells, we infected ELP3 knockout (KO) HeLa HSP27-GFP cells and control HeLa HSP27-GFP cells with IAV. Cells were collected at 16h post-infection and viral titres were determined and calculated by plaque assay.

For the second part of our study, our hypothesis was based on the fact that after infection, some TMEs were overexpressed 2 hpi, which might mean that the virus might benefit from the increased expression of these enzymes. To observe if that was the case, we inhibited the expression of ELP3, the catalytic subunit of the elongator complex, to observe whether changes in virus propagation occurred (Figure 10).

Therefore, to conduct our experiments we utilized an ELP3 KO cell line, which was developed in our laboratory. The KO of ELP3 was induced in HeLa cells expressing the fluorescent reporter HSP27-GFP, and the creation and establishment of this stable cell line was made using the CRISPR/Cas9 system[102].

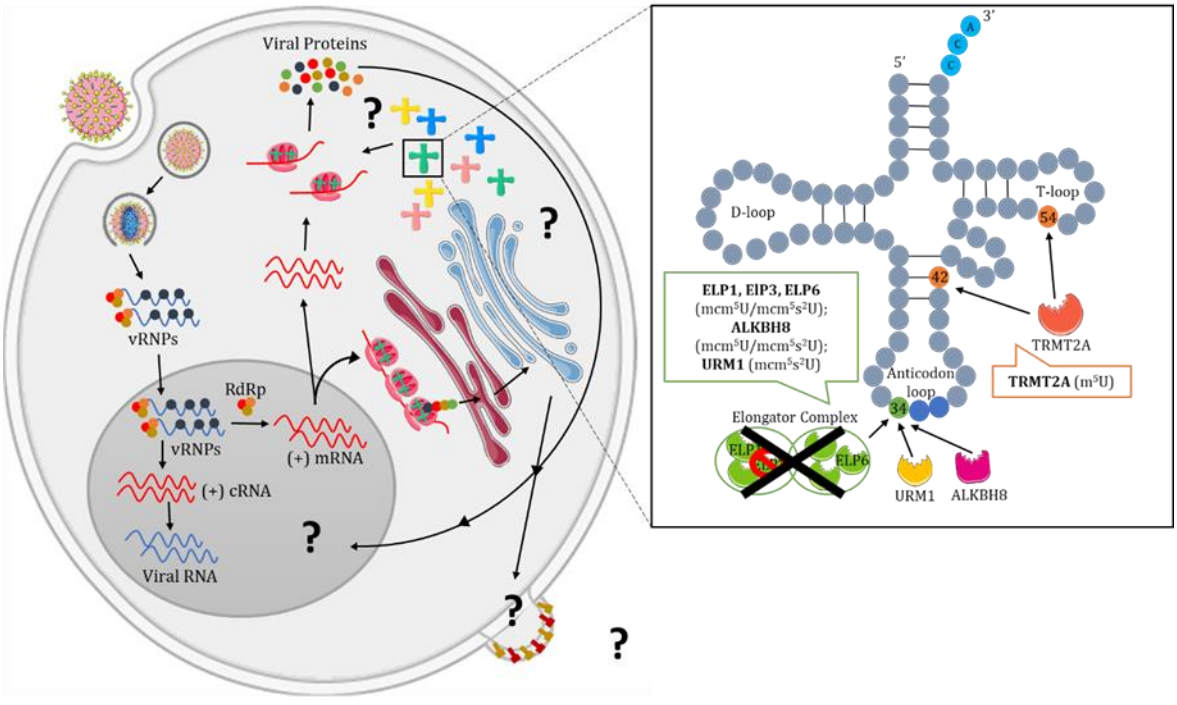

Figure 10. tRNA secondary cloverleaf structure and the potential effects of ELP3 absence in the IAV life-cycle. The elongator complex catalyses one of the first modifications in the wobble position located in the anticodon loop. ELP3 is the catalytic subunit of the complex and one of its most important subunits. By inducing the KO of ELP3 in HeLa cells, we want to evaluate changes in viral particle production when compared to a control cell line.

Confirmation of ELP3 KO

First and foremost, before advancing in our experimental procedure, we wanted to make sure that the KO of ELP3 was indeed effective. We tested this via western blot analysis with staining with an anti-ELP3 primary antibody. The results, presented in Figure 11, suggest that the KO was indeed effective in the intended cell lines.

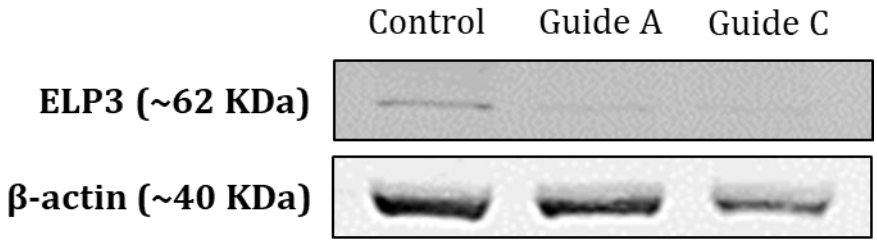

Figure 11. Western blot to confirm ELP3 KO in HeLa cells. Western blot analysis showing an effective KO of ELP3 in HeLa guide cells. ELP3 was only detected in HeLa control cells. β-actin was used as the loading control.

During the establishment of the ELP3 KO cell line, HeLa HSP27-GFP cells were transfected with three different guides, A, B and C, with the same treatment and procedure being applied to each of them. ELP3 was only detected as a 62 kDA band in HeLa HSP27-GFP cells transfected with scramble controls, while among the tested guides, C was the one which presented the highest KO rate and was the one we chose to utilize for the rest of the experiment. Before usage however, single cell selection was performed using puromycin in a concentration of 2 μg/mL, and once the final KO cells were obtained, they were infected with IAV for further analysis', such as, identification of NP intracellular localization 16 hpi and measurement of viral production.

Confirmation of Infection

As mentioned, ELP3 KO HeLa HSP27-GFP cells and control HeLa HSP27-GFP cells were infected with IAV, and supernatants were collected at 16h post-infection. Before performing the plaque assays, we wanted to confirm whether infection was successful. For that, we performed western blot and immunofluorescence assays.

To conduct our analysis by western blot, we used the pellets that were collected upon infection of HeLa HSP27-GFP cells with PR8, to extract total protein using ELB supplemented with protease inhibitors. Quantification was then performed using the Pierce™ Bovine Serum Albumin (BCA) Protein Assay Kit. Protein samples were diluted in 6x loading buffer and ran by SDS-PAGE. Membranes were visualized using the Odyssey Imaging System, after incubation with anti-NP primary antibody. Our results, as shown in Figure 12, indicate presence of NP in IAV infected cells 16 hpi, while mock-infected cells didn't show presence of the viral protein, suggesting that infection was indeed successful.

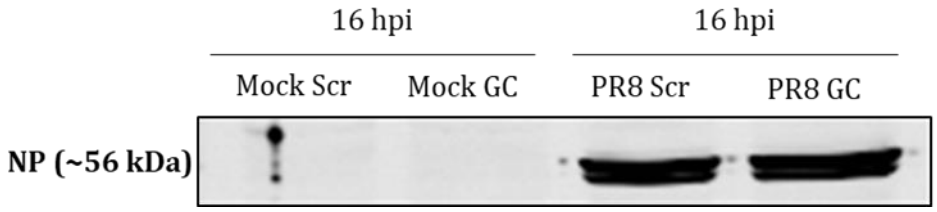

Figure 12. Confirmation of IAV infection via Western Blot analysis. The IAV viral protein NP is detected in IAV infected cells while no traces of the protein are detected in mock-infected cells.

Absence of ELP3 reduces viral propagation

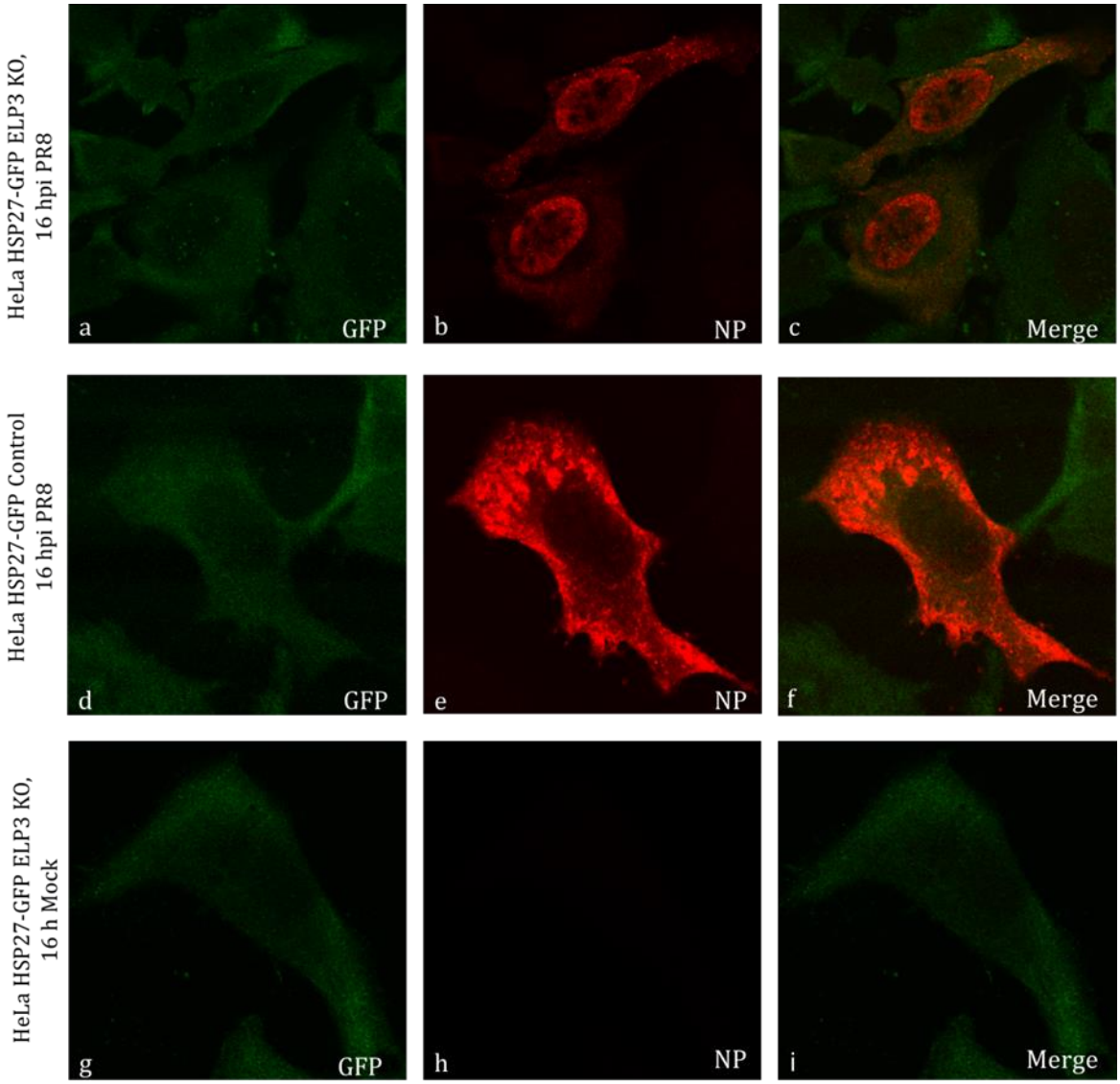

Figure 13. The absence of ELP3 results in a slower infection. Confocal microscope images of (a,b and c) HeLa HSP27-GFP Guide C (ELP3 KO) cells 16h post-infection, (d,e and f) HeLa HSP27-GFP Control cells 16h post-infection and (g, h and i) HeLa HSP27-GFP Guide C (ELP3 KO) cells 16h mock-infected. Viral protein NP is shown in red.

Simultaneously, we also performed an analysis by confocal microscopy which, not only confirmed that infection was indeed successful, corroborating the results obtained by western blot analysis but, more interestingly, as shown in Figure 13, that ELP3 KO cells present a drastic delay in the viral life-cycle as, at 16h post-infection, viral NP is still present at the nucleus while in Control cells, viral NP is already near the cell membrane, indicating that the virus is about to be released from the cells, as was expected.

After confirmation of infection we performed plaque assays, which are used to determine viral titre as plaque forming units per milliliter (pfu/ml).

Regarding the plaque assays, MDCK monolayers were infected with the supernatants that were collected during the infection protocol, and for each condition (Control Mock, Control PR8, ELP3 KO Mock and ELP3 KO PR8) we prepared a dilution set (-1 to -5 for infected conditions, -1 for mock conditions). At the end of the protocol, we incubated the wells, overnight, with 0.1% toluidine blue in 4% PFA which allowed us to count the plaques formed in each well. The best dilution was the one that had more and better visible plaques, which in the first replica (n1) corresponds to the -3 dilution, and the -2 dilution in the second replica (n2), as observed in Figure 14.

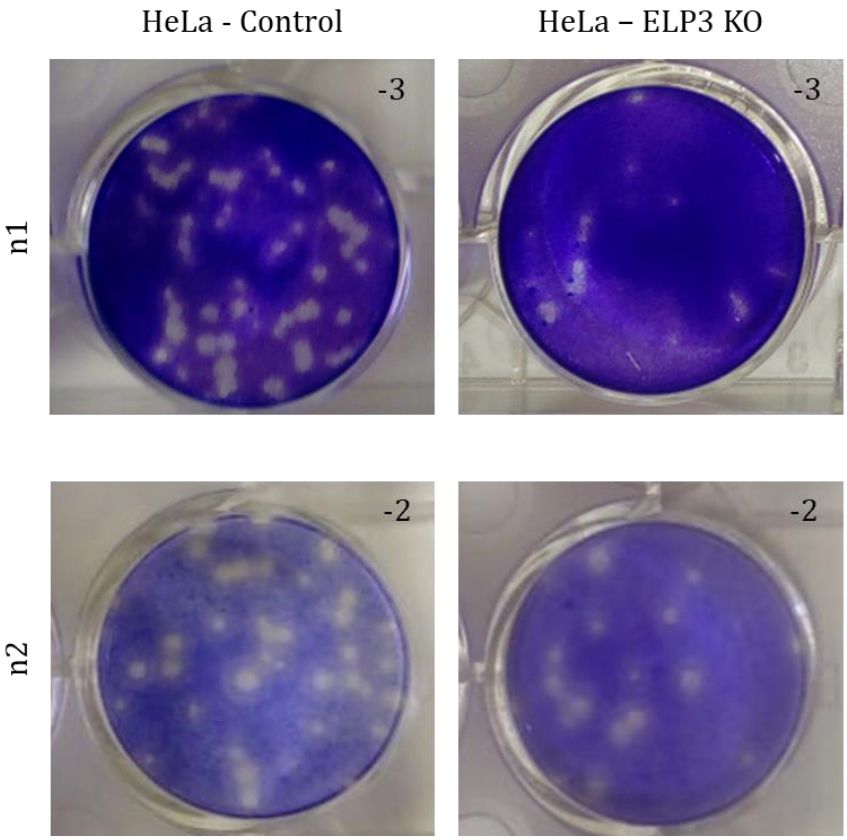

Figure 14. Plaque assay quantification. As observed, in both replicas', HeLa HSP27-GFP control cells produced a higher number of plaques when compared to HeLa HSP27-GFP ELP3 KO cells.

After counting the plaques, we performed the necessary calculations in order to determine the virus titre of each condition. The obtained results, as shown in Figure 15, showcase that viral production was highly reduced in the absence of ELP3. While performing the different replicas' we adjusted the number of seeded cells according to the cells growth rate, hence why the results of different replicas are presented separately.

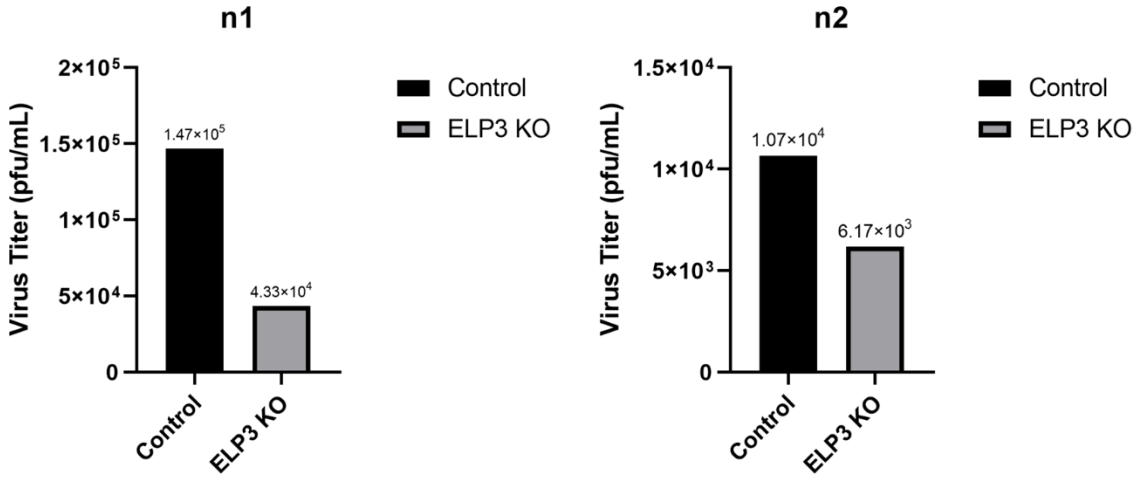

Figure 15. Virus particles production by the infected HeLa HSP27-GFP control cells and HeLa HSP27-GFP ELP3 KO cells. In the performed replicas, HeLa HSP27-GFP control cells formed a higher number of plaques when compared to HeLa HSP27-GFP ELP3 KO cells. N1 refers to the first replica, while n2 refers to the second replica.

As previously mentioned, the elongator complex mediates the modification of the wobble position in some types of tRNAs, thus promoting translation efficiency. Yeast cells lacking the ELP3 subunit of the complex, have been shown to be less resistant to stress[103], when compared with cells that possess modifications induced by this complex, and one of the reasons this might happen is because cells lacking ELP3 aren't able to modify the uridine wobble nucleoside of tRNAs[103]. Fernández-Vázquez et al.[103], have shown that the absence of ELP3 leads to a non-functional elongator complex, resulting in translation inefficiency and the surge of stress phenotypes[103]. Furthermore, ELP3 has also been associated with neurological disorders, such as motor neuron degeneration in amyotrophic lateral sclerosis[77]. Simpson et al.[77], showed that ELP3 is important for neuron functioning and survival, since drosophila and zebrafish embryos lacking ELP3 develop motor axonal abnormalities[54,77]. These studies showcase that ELP3 is an extremely important TME, and its absence can often times lead to poor functioning of the cell, and in more extreme cases, to the development of diseases. However, this enzyme hasn't been thoroughly studied in an infection context with neither IAV or any other virus. Our results show that viral production was highly reduced in the absence of ELP3 and infected ELP3 KO cells present a drastic delay in the viral life-cycle as, at 16h post-infection, viral NP is still present at the nucleus. These results suggest that not only is ELP3 involved in the development of neurological disorders, as shown by Simpson et al.[77] but it may also play a relevant role on the IAV life-cycle.

As shown by Fernández-Vázquez et al.[103], absence of ELP3 can lead to the development of stress phenotypes[103]. This can mean that the obtained reduction in viral production can be caused by the stress the cell is exposed to, due to the absence of ELP3, and not because ELP3 is important in the viral life-cycle. To test this, a possible test to perform in the future will be to induce overexpression of ELP3 in HeLa HSP27-GFP cells and observe if viral production increases. If that is the case, it might definitely indicate that ELP3 does play an extremely important role in the IAV life-cycle. Another test to further corroborate our analysis could be a functional analysis to see whether tRNAs were, in fact, missing the modifications induced by ELP3. This test could show us that the elongator complex is indeed non-functional in the absence of ELP3. Performing plaque assays using different strains and types of IAV, and even other viruses, may also provide a better understanding of the role of ELP3 in viral infection. If absence of ELP3 leads to a generalized reduction in viral particle production, we can maybe identify ELP3 as a potential target for antiviral treatment.

CONCLUSIONS AND FINAL REMARKS

Influenza A Virus infection impact on the pool of TMEs of the host

During its life-cycle IAV takes control of the host cell machinery to produce its own viral proteins. Pavon-Eternod et al.[90], found that in its life-cycle, IAV interacts with the tRNA population of the host cell translation machinery. In this study, while the total tRNA population remained unchanged upon IAV infection, the polysome-associated tRNA population changed substantially in a virus-specific way, indicating that the virus altered and optimized the hosts' tRNA population to better match IAV codon usage. Our results, although preliminary, indicate that not only does IAV interact with the tRNA population, but it also interferes with the TME population of host cells. TMEs are enzymes that post-transcriptionally modify tRNAs in order to increase translation efficiency. Some TMEs (ELP1, ELP3, ELP6, ALKBH8 and TRMT2A) appear to be overexpressed two hours after infection with IAV, while no changes were detected in other time points. These results must be complemented with further replicates, given that some variance in expression values was observed during the experimental procedure. Other avenues of investigation should also be approached, namely trying to get an expression profile of other TMEs in the multiple time points of infection.

Effect of the lack of a TME on IAV propagation

In order to determine whether the lack of one of these TMEs, more specifically ELP3, would influence the viral particle production by the infected cells, we infected HeLa HSP27-GFP ELP3 KO cells and HeLa HSP27-GFP control cells with IAV. Cells were collected at 16h post-infection and viral titres were determined by plaque assay. Our preliminary results show that viral production was highly reduced in the absence of ELP3, and interestingly, as observed via immunofluorescence, ELP3 KO cells present a significant delay in the viral life-cycle as, at 16 hpi, the viral genome is still present at the nucleus, suggesting a relevant role for ELP3 on the IAV life-cycle. These results must also be complemented with more replicates to get a more reliable analysis, and further testing is also required. One proposed test is to overexpress ELP3 and observe whether viral production increases or not. If that is indeed the case, ELP3 may be seen as a potential target for antiviral treatment. In the near future, we plan on performing the same experimental procedure using different strains of IAV, and potentially other viruses, to get a better understanding of the role of ELP3 in viral infection.

Publications resulting from this work

Nunes, A.*, Ribeiro, D.R*., Marques, M., Santos, M. Ribeiro, D.# and Soares, A.R.#, "tRNA epitranscriptome regulation during viral infections", *equal contribution, #equal contribution, manuscript in preparation to be submitted to Trends in Cell Biology.

REFERENCES

1. Noda T. Native morphology of influenza virions. *Front Microbiol*. 2012;2(JAN):1-5. doi:10.3389/fmicb.2011.00269
2. Paget J, Spreeuwenberg P, Charu V, et al. Global mortality associated with seasonal influenza epidemics: New burden estimates and predictors from the GLaMOR Project. *J Glob Health*. 2019;9(2):020421. doi:10.7189/jogh.09.020421
3. Opitz L, Zimmermann A, Lehmann S, et al. Capture of cell culture-derived influenza virus by lectins: Strain independent, but host cell dependent. *J Virol Methods*. 2008;154(1-2):61-68. doi:10.1016/j.jviromet.2008.09.004
4. Baltimore D. Expression of animal virus genomes. *Bacteriol Rev*. 1971;35(3):235-241.
5. Taubenberger JK, Morens DM. The Pathology of Influenza Virus Infections. *Annu Rev Pathol Mech Dis*. 2008;3(1):499-522. doi:10.1146/annurev.pathmechdis.3.121806.154316
6. Paules C, Subbarao K. Influenza. *Lancet*. 2017;390(10095):697-708. doi:10.1016/S0140-6736(17)30129-0
7. Hutchinson EC. Influenza Virus. *Trends Microbiol*. 2018;26(9):809-810. doi:10.1016/j.tim.2018.05.013
8. Briedis DJ. Influenza Viruses. In: *Fundamentals of Molecular Virology*. 2nd ed. Wiley; 2011.
9. Killingley B, Nguyen-Van-Tam J. Routes of influenza transmission. *Influenza Other Respi Viruses*. 2013;7:42-51. doi:10.1111/irv.12080
10. Cowling BJ, Ip DKM, Fang VJ, et al. Aerosol transmission is an important mode of influenza A virus spread. *Nat Commun*. 2013;4(1):1935. doi:10.1038/ncomms2922
11. Tellier R. Review of aerosol transmission of influenza A virus. *Emerg Infect Dis*. 2006;12(11):1657-1662. doi:10.3201/eid1211.060426
12. Nikitin N, Petrova E, Trifonova E, Karpova O. Influenza Virus Aerosols in the Air and Their Infectiousness. *Adv Virol*. 2014;2014:1-6. doi:10.1155/2014/859090
13. Anderson CS, Ortega S, Chaves FA, et al. Natural and directed antigenic drift of the H1 influenza virus hemagglutinin stalk domain. *Sci Rep*. 2017;7(1):14614. doi:10.1038/s41598-017-14931-7
14. Webster RG, Govorkova EA. Continuing challenges in influenza. *Ann N Y Acad Sci*. 2014;1323(1):115-139. doi:10.1111/nyas.12462
15. Houser K, Subbarao K. Influenza vaccines: Challenges and solutions. *Cell Host Microbe*. 2015;17(3):295-300. doi:10.1016/j.chom.2015.02.012
16. Doyle JD, Chung JR, Kim SS, et al. Interim Estimates of 2018-19 Seasonal Influenza Vaccine Effectiveness - United States, February 2019. *MMWR Morb Mortal Wkly Rep*. 2019;68(6):135-139. doi:10.15585/mmwr.mm6806a2
17. Mckimm-Breschkin JL. Influenza neuraminidase inhibitors: Antiviral action and mechanisms of resistance. *Influenza Other Respi Viruses*. 2013;7(1 SUPPL.1):25-36. doi:10.1111/irv.12047
18. Hari Narayana Moorthy NS, Poongavanam V, Pratheepa V. Viral M2 ion channel protein: A promising target for anti-influenza drug discovery. *Mini-Reviews Med Chem*. 2014;14(10):819-830. doi:10.2174/1389557514101410201508 22

19. Winter G, Fields S. Nucleic Acids Research Nucleotide sequence of hunan influenza A/PR/8/34 segment 2. 1982;(6):2135-2143. https://www.ncbi.nlm.nih.gov/pmc/articles/PMC320594/pdf/nar00375-0307.pdf.
20. Bouvier NM, Palese P. The biology of influenza viruses. *Vaccine*. 2008;26(SUPPL. 4). doi:10.1016/j.vaccine.2008.07.039
21. Lakdawala SS, Nair N, Hutchinson E. Educational material about influenza viruses. *Viruses*. 2019;11(3):1-9. doi:10.3390/v11030231
22. Das K, Aramini JM, Ma L-C, Krug RM, Arnold E. Structures of influenza A proteins and insights into antiviral drug targets. *Nat Struct Mol Biol*. 2010;17(5):530-538. doi:10.1038/nsmb.1779
23. Samji T. Influenza A - Understanding the Viral Life Cycle. *YALE J Biol Med*. 2009;82:153-159.
24. Watanabe K, Shimizu T, Noda S, Tsukahara F, Maru Y, Kobayashi N. Nuclear export of the influenza virus ribonucleoprotein complex: Interaction of Hsc70 with viral proteins M1 and NS2. *FEBS Open Bio*. 2014;4:683-688. doi:10.1016/j.fob.2014.07.004
25. Reich S, Guilligay D, Pflug A, et al. Structural insight into cap-snatching and RNA synthesis by influenza polymerase. *Nature*. 2014;516(7531):361-366. doi:10.1038/nature14009
26. Dou D, Revol R, Östbye H, Wang H, Daniels R. Influenza A virus cell entry, replication, virion assembly and movement. *Front Immunol*. 2018;9(JUL):1-17. doi:10.3389/fimmu.2018.01581
27. Turrell L, Lyall JW, Tiley LS, Fodor E, Vreede FT. The role and assembly mechanism of nucleoprotein in influenza A virus ribonucleoprotein complexes. *Nat Commun*. 2013;4(0):1-24. doi:10.1038/ncomms2589
28. Hutchinson EC, Fodor E. Nuclear import of the influenza A virus transcriptional machinery. *Vaccine*. 2012;30(51):7353-7358. doi:10.1016/j.vaccine.2012.04.085
29. Hutchinson EC, Fodor E. Transport of the influenza virus genome from nucleus to nucleus. *Viruses*. 2013;5(10):2424-2446. doi:10.3390/v5102424
30. Rossman JS, Lamb RA. Influenza virus assembly and budding. *Virology*. 2011;411(2):229-236. doi:10.1016/j.virol.2010.12.003
31. Atkin-Smith GK, Duan M, Chen W, Poon IKH. The induction and consequences of Influenza A virus-induced cell death. *Cell Death Dis*. 2018;9(10). doi:10.1038/s41419-018-1035-6
32. Fujikura D, Miyazaki T. Programmed cell death in the pathogenesis of influenza. *Int J Mol Sci*. 2018;19(7):1-14. doi:10.3390/ijms19072065
33. Chen X, Liu S, Goraya MU, Maarouf M, Huang S, Chen JL. Host immune response to influenza A virus infection. *Front Immunol*. 2018;9(MAR):1-13. doi:10.3389/fimmu.2018.00320
34. Kreijtz JHCM, Fouchier RAM, Rimmelzwaan GF. Immune responses to influenza virus infection. *Virus Res*. 2011;162(1-2):19-30. doi:10.1016/j.virusres.2011.09.022
35. Biondo C, Lentini G, Beninati C, Teti G. The dual role of innate immunity during influenza. *Biomed J*. 2019;42(1):8-18. doi:10.1016/j.bj.2018.12.009
36. van de Sandt CE, Kreijtz JHCM, Rimmelzwaan GF. Evasion of Influenza A Viruses from Innate and Adaptive Immune Responses. *Viruses*. 2012;4(9):1438-1476. doi:10.3390/v4091438

37. Koh CS, Sarin LP. Transfer RNA modification and infection – Implications for pathogenicity and host responses. *Biochim Biophys Acta - Gene Regul Mech*. 2018;1861(4):419-432. doi:10.1016/j.bbagrm.2018.01.015
38. Raina M, Ibba M. tRNAs as regulators of biological processes. *Front Genet*. 2014;5(JUN):1-14. doi:10.3389/fgene.2014.00171
39. Watson JD, Baker TA, Bell SP, Gann A, Levine M, Losick R. *Molecular Biology of the Gene*. 7th ed. Pearson; 2013.
40. Phizicky EM, Hopper AK. tRNA biology charges to the front. *Genes Dev*. 2010;24(17):1832-1860. doi:10.1101/gad.1956510
41. Turowski TW, Tollervey D. Transcription by RNA polymerase III: Insights into mechanism and regulation. *Biochem Soc Trans*. 2016;44(5):1367-1375. doi:10.1042/BST20160062
42. Spears JL, Rubio MAT, Sample PJ, Alfonzo JD. tRNA Biogenesis and Processing. In: ; 2012:99-121. doi:10.1007/978-3-642-28687-2_5
43. Pang YLJ, Poruri K, Martinis SA. tRNA synthetase: tRNA aminoacylation and beyond. *Wiley Interdiscip Rev RNA*. 2014;5(4):461-480. doi:10.1002/wrna.1224
44. Schimmel P. The emerging complexity of the tRNA world: mammalian tRNAs beyond protein synthesis. *Nat Rev Mol Cell Biol*. 2018;19(1):45-58. doi:10.1038/nrm.2017.77
45. Lodish H, Berk A, Zipursky S. Section 4.4, The Three Roles of RNA in Protein Synthesis. In: *Molecular Cell Biology*. 4th ed. New York: W. H. Freeman; 2000. https://www.ncbi.nlm.nih.gov/books/NBK21603/.
46. Pak D, Root-Bernstein R, Burton ZF. tRNA structure and evolution and standardization to the three nucleotide genetic code. *Transcription*. 2017;8(4):205-219. doi:10.1080/21541264.2017.1318811
47. Hou Y-M. CCA addition to tRNA: Implications for tRNA quality control. *IUBMB Life*. 2010;23(1):NA-NA. doi:10.1002/iub.301
48. Hardt WD, Schlegl J, Erdmann VA, Hartmann RK. Role of the D Arm and the Anticodon Arm in tRNA Recognition by Eubacterial and Eukaryotic RNase P Enzymes. *Biochemistry*. 1993;32(48):13046-13053. doi:10.1021/bi00211a014
49. Puglisi JD, Pütz J, Florentz C, Giegé R. Influence of tRNA tertiary structure and stability on aminoacylation by yeast aspartyl-tRNA synthetase. *Nucleic Acids Res*. 1993;21(1):41-49. doi:10.1093/nar/21.1.41
50. Chan CW, Chetnani B, Mondragón A. Structure and function of the T-loop structural motif in noncoding RNAs. *Wiley Interdiscip Rev RNA*. 2013;4(5):507-522. doi:10.1002/wrna.1175
51. Agris PF, Eruysal ER, Narendran A, Väre VYP, Vangaveti S, Ranganathan S V. Celebrating wobble decoding: Half a century and still much is new. *RNA Biol*. 2018;15(4-5):537-553. doi:10.1080/15476286.2017.1356562
52. Rozov A, Demeshkina N, Khusainov I, Westhof E, Yusupov M, Yusupova G. Novel base-pairing interactions at the tRNA wobble position crucial for accurate reading of the genetic code. *Nat*

Commun. 2016;7:1-10. doi:10.1038/ncomms10457

53. Agris PF, Vendeix FAP, Graham WD. tRNA's Wobble Decoding of the Genome: 40 Years of Modification. *J Mol Biol*. 2007;366(1):1-13. doi:10.1016/j.jmb.2006.11.046
54. Pereira M, Francisco S, Varanda AS, Santos M, Santos MAS, Soares AR. Impact of tRNA modifications and tRNA-modifying enzymes on proteostasis and human disease. *Int J Mol Sci*. 2018;19(12). doi:10.3390/ijms19123738
55. Zamudio GS, José M V. On the uniqueness of the standard genetic code. *Life*. 2017;7(1):7. doi:10.3390/life7010007
56. Helm M, Alfonzo JD. Posttranscriptional RNA modifications: Playing metabolic games in a cell's chemical legoland. *Chem Biol*. 2014;21(2):174-185. doi:10.1016/j.chembiol.2013.10.015
57. Oberbauer V, Schaefer MR. tRNA-derived small RNAs: Biogenesis, modification, function and potential impact on human disease development. *Genes (Basel)*. 2018;9(12). doi:10.3390/genes9120607
58. Novoa EM, Pavon-Eternod M, Pan T, Ribas De Pouplana L. A role for tRNA modifications in genome structure and codon usage. *Cell*. 2012;149(1):202-213. doi:10.1016/j.cell.2012.01.050
59. Lorenz C, Lünse C, Mörl M. tRNA Modifications: Impact on Structure and Thermal Adaptation. *Biomolecules*. 2017;7(4):35. doi:10.3390/biom7020035
60. Boccaletto P, MacHnicka MA, Purta E, et al. MODOMICS: A database of RNA modification pathways. 2017 update. *Nucleic Acids Res*. 2018;46(D1):D303-D307. doi:10.1093/nar/gkx1030
61. Tuorto F, Lyko F. Genome recoding by tRNA modifications. *Open Biol*. 2016;6(12):0-2. doi:10.1098/rsob.160287
62. Pan T. Modifications and functional genomics of human transfer RNA. *Cell Res*. 2018;28(4):395-404. doi:10.1038/s41422-018-0013-y
63. Ranjan N, Rodnina M V. TRNA wobble modifications and protein homeostasis. *Translation*. 2016;4(1):1-11. doi:10.1080/21690731.2016.1143076
64. Yu F, Tanaka Y, Yamashita K, et al. Molecular basis of dihydrouridine formation on tRNA. *Proc Natl Acad Sci U S A*. 2011;108(49):19593-19598. doi:10.1073/pnas.1112352108
65. Duechler M, Leszczyńska G, Sochacka E, Nawrot B. Nucleoside modifications in the regulation of gene expression: focus on tRNA. *Cell Mol Life Sci*. 2016;73(16):3075-3095. doi:10.1007/s00018-016-2217-y
66. Väre VYP, Eruysal ER, Narendran A, Sarachan KL, Agris PF. Chemical and conformational diversity of modified nucleosides affects tRNA structure and function. *Biomolecules*. 2017;7(1):1-32. doi:10.3390/biom7010029
67. Shippy DC, Fadl AA. tRNA modification enzymes gidA and mnmE: Potential role in virulence of bacterial pathogens. *Int J Mol Sci*. 2014;15(10):18267-18280. doi:10.3390/ijms151018267
68. Ferré-D'Amaré AR. RNA-modifying enzymes. *Curr Opin Struct Biol*. 2003;13(1):49-55. doi:10.1016/S0959-440X(02)00002-7
69. Chou HJ, Donnard E, Gustafsson HT, Garber M, Rando OJ. Transcriptome-wide Analysis of Roles

for tRNA Modifications in Translational Regulation. *Mol Cell*. 2017;68(5):978-992.e4. doi:10.1016/j.molcel.2017.11.002

70. Karlsborn T, Tükenmez H, Mahmud AKMF, Xu F, Xu H, Byström AS. Elongator, a conserved complex required for wobble uridine modifications in Eukaryotes. *RNA Biol*. 2014;11(12):1519-1528. doi:10.4161/15476286.2014.992276
71. Svejstrup JQ. Elongator complex: how many roles does it play? *Curr Opin Cell Biol*. 2007;19(3):331-336. doi:10.1016/j.ceb.2007.04.005
72. Versées W, De Groeve S, Van Lijsebettens M. Elongator, a conserved multitasking complex? *Mol Microbiol*. 2010;76(5):1065-1069. doi:10.1111/j.1365-2958.2010.07162.x
73. Glatt S, Zabel R, Kolaj-Robin O, et al. Structural basis for tRNA modification by Elp3 from Dehalococcoides mccartyi. *Nat Struct Mol Biol*. 2016;23(9):794-802. doi:10.1038/nsmb.3265
74. Ladang A, Rapino F, Heukamp LC, et al. Elp3 drives Wnt-dependent tumor initiation and regeneration in the intestine. *J Exp Med*. 2015;212(12):2057-2075. doi:10.1084/jem.20142288
75. Laguesse S, Creppe C, Nedialkova DD, et al. A Dynamic Unfolded Protein Response Contributes to the Control of Cortical Neurogenesis. *Dev Cell*. 2015;35(5):553-567. doi:10.1016/j.devcel.2015.11.005
76. Bento-Abreu A, Jager G, Swinnen B, et al. Elongator subunit 3 (ELP3) modifies ALS through tRNA modification. *Hum Mol Genet*. 2018;27(7):1276-1289. doi:10.1093/hmg/ddy043
77. Simpson CL, Lemmens R, Miskiewicz K, et al. Variants of the elongator protein 3 (ELP3) gene are associated with motor neuron degeneration. *Hum Mol Genet*. 2009;18(3):472-481. doi:10.1093/hmg/ddn375
78. Leidel S, Pedrioli PGA, Bucher T, et al. Ubiquitin-related modifier Urm1 acts as a sulphur carrier in thiolation of eukaryotic transfer RNA. *Nature*. 2009;458(7235):228-232. doi:10.1038/nature07643
79. Van Der Veen AG, Schorpp K, Schlieker C, et al. Role of the ubiquitin-like protein Urm1 as a noncanonical lysine-directed protein modifier. *Proc Natl Acad Sci U S A*. 2011;108(5):1763-1770. doi:10.1073/pnas.1014402108
80. Xu J, Zhang J, Wang L, et al. Solution structure of Urm1 and its implications for the origin of protein modifiers. *Proc Natl Acad Sci U S A*. 2006;103(31):11625-11630. doi:10.1073/pnas.0604876103
81. Songe-Moller L, van den Born E, Leihne V, et al. Mammalian ALKBH8 Possesses tRNA Methyltransferase Activity Required for the Biogenesis of Multiple Wobble Uridine Modifications Implicated in Translational Decoding. *Mol Cell Biol*. 2010;30(7):1814-1827. doi:10.1128/mcb.01602-09
82. Van Den Born E, Vågbø CB, Songe-Møller L, et al. ALKBH8-mediated formation of a novel diastereomeric pair of wobble nucleosides in mammalian tRNA. *Nat Commun*. 2011;2(1):172-177. doi:10.1038/ncomms1173
83. Shimada K, Nakamura M, Anai S, et al. A novel human AIkB homologue, ALKBH8, contributes to

human bladder cancer progression. *Cancer Res*. 2009;69(7):3157-3164. doi:10.1158/0008-5472.CAN-08-3530

84. Hicks DG, Janarthanan BR, Vardarajan R, et al. The expression of TRMT2A, a novel cell cycle regulated protein, identifies a subset of breast cancer patients with HER2 over-expression that are at an increased risk of recurrence. *BMC Cancer*. 2010;10. doi:10.1186/1471-2407-10-108
85. Chang YH, Nishimura S, Oishi H, Kelly VP, Kuno A, Takahashi S. TRMT2A is a novel cell cycle regulator that suppresses cell proliferation. *Biochem Biophys Res Commun*. 2019;508(2):410-415. doi:10.1016/j.bbrc.2018.11.104
86. Towns WL, Begley TJ. Transfer RNA methytransferases and their corresponding modifications in budding yeast and humans: Activities, predications, and potential roles in human health. *DNA Cell Biol*. 2012;31(4):434-454. doi:10.1089/dna.2011.1437
87. Albers S, Czech A. Exploiting tRNAs to boost virulence. *Life*. 2016;6(1). doi:10.3390/life6010004
88. Marques M, Ramos B, Soares A, Ribeiro D. Cellular Proteostasis During Influenza A Virus Infection—Friend or Foe? *Cells*. 2019;8(3):228. doi:10.3390/cells8030228
89. van Weringh A, Ragonnet-Cronin M, Pranckeviciene E, Pavon-Eternod M, Kleiman L, Xia X. HIV-1 Modulates the tRNA Pool to Improve Translation Efficiency. *Mol Biol Evol*. 2011;28(6):1827-1834. doi:10.1093/molbev/msr005
90. Pavon-Eternod M, David A, Dittmar K, et al. Vaccinia and influenza A viruses select rather than adjust tRNAs to optimize translation. *Nucleic Acids Res*. 2013;41(3):1914-1921. doi:10.1093/nar/gks986
91. Hendrix RW. *Lesser Known Large DsDNA Viruses, Current Topics in Microbiology and Immunology*. Vol 328. (Van Etten JL, ed.). Berlin, Heidelberg: Springer Berlin Heidelberg; 2009. doi:10.1007/978-3-540-68618-7
92. Torres AG, Batlle E, Ribas de Pouplana L. Role of tRNA modifications in human diseases. *Trends Mol Med*. 2014;20(6):306-314. doi:10.1016/j.molmed.2014.01.008
93. Cohen JS, Srivastava S, Farwell KD, et al. ELP2 is a novel gene implicated in neurodevelopmental disabilities. *Am J Med Genet Part A*. 2015;167(6):1391-1395. doi:10.1002/ajmg.a.36935
94. Abbasi-Moheb L, Mertel S, Gonsior M, et al. Mutations in NSUN2 Cause Autosomal- Recessive Intellectual Disability. *Am J Hum Genet*. 2012;90(5):847-855. doi:10.1016/j.ajhg.2012.03.021
95. Palmer CJ, Bruckner RJ, Paulo JA, et al. Cdkal1, a type 2 diabetes susceptibility gene, regulates mitochondrial function in adipose tissue. *Mol Metab*. 2017;6(10):1212-1225. doi:10.1016/j.molmet.2017.07.013
96. Wei F-Y, Suzuki T, Watanabe S, et al. Deficit of tRNALys modification by Cdkal1 causes the development of type 2 diabetes in mice. *J Clin Invest*. 2011;121(9):3598-3608. doi:10.1172/JCI58056
97. Huang S, Sun B, Xiong Z, et al. The dysregulation of tRNAs and tRNA derivatives in cancer. *J Exp Clin Cancer Res*. 2018;37(1):101. doi:10.1186/s13046-018-0745-z
98. Rapino F, Delaunay S, Zhou Z, Chariot A, Close P. tRNA Modification: Is Cancer Having a Wobble?

Trends in Cancer. 2017;3(4):249-252. doi:10.1016/j.trecan.2017.02.004

99. Guy MP, Shaw M, Weiner CL, et al. Defects in tRNA Anticodon Loop 2′- O -Methylation Are Implicated in Nonsyndromic X-Linked Intellectual Disability due to Mutations in FTSJ1. *Hum Mutat*. 2015;36(12):1176-1187. doi:10.1002/humu.22897
100. Luo L, Han W, Du J, et al. Chenodeoxycholic acid from bile inhibits influenza A virus replication via blocking nuclear export of viral ribonucleoprotein complexes. *Molecules*. 2018;2009. doi:10.3390/molecules23123315
101. Duchon AA, St. Gelais C, Titkemeier N, Hatterschide J, Wu L, Musier-Forsyth K. HIV-1 Exploits a Dynamic Multi-aminoacyl-tRNA Synthetase Complex To Enhance Viral Replication. Sundquist WI, ed. *J Virol*. 2017;91(21). doi:10.1128/JVI.01240-17
102. Tycko J, Myer VE, Hsu PD. Methods for Optimizing CRISPR-Cas9 Genome Editing Specificity. *Mol Cell*. 2016;63(3):355-370. doi:10.1016/j.molcel.2016.07.004
103. Fernández-Vázquez J, Vargas-Pérez I, Sansó M, et al. Modification of tRNALys UUU by Elongator Is Essential for Efficient Translation of Stress mRNAs. Madhani HD, ed. *PLoS Genet*. 2013;9(7):e1003647. doi:10.1371/journal.pgen.1003647